T.C.
DOKUZ EYLUL UNIVERSITY
IZMIR INTERNATIONAL
BIOMEDICINE AND GENOME
INSTITUTE

INVESTIGATION OF CHROMATIN-CHROMATIN INTERACTION OF GLIOMA RISK LOCUS AT 8q24.21 by CHROMOSOME CONFORMATION CAPTURE TECHNIQUES AND EFFECTS OF IDH MUTATIONS

TUTKU YARAŞ

MOLECULAR BIOLOGY AND GENETICS

MASTER'S THESIS

İZMİR – 2019

THESIS CODE: DEU.HSI.MSc-2016850010

T.C.
DOKUZ EYLUL UNIVERSITY IZMIR
INTERNATIONAL BIOMEDICINE AND GENOME
INSTITUTE

INVESTIGATION OF CHROMATIN-CHROMATIN INTERACTION OF GLIOMA RISK LOCUS AT 8q24.21 by CHROMOSOME CONFORMATION CAPTURE TECHNIQUES AND EFFECTS OF IDH MUTATIONS

MOLECULAR BIOLOGY AND GENETICS

MASTER'S THESIS

TUTKU YARAŞ

Assoc. Prof. Yavuz OKTAY

(This project was funded by TUBITAK. The project number was 214S097)

THESIS CODE: DEU.HSI.MSc-2016850010

Dokuz Eylül Üniversitesi İzmir Uluslararası Biyotıp ve Genom Enstitüsü Genom Bilimleri ve Moleküler Biyoteknoloji Anabilim Dalı, Moleküler Byoloji ve Genetik Yüksek Lisans programı öğrencisi "Kromozom Konformasyonu Yakalama Teknikleriyle 8q24.21 Bölgesindeki Glioma Risk-Lokus Alanlarının Kromatin-Kromatin Etkileşimlerinin Belirlenmesi Ve IDH Mutasyonunun Etkisinin Araştırılması' konulu Doktora/Yüksek Lisans tezini 12/06/2019 tarihinde başarılı olarak tamamlamıştır.

BAŞKAN
Doktor Öğretim Üyesi Yavuz OKTAY

ÜYE
Prof. Dr. Şermin GENÇ

ÜYE
Doç. Dr. Özden YALÇIN ÖZUYSAL

YEDEK ÜYE

Doç. Dr. Hatice Güneş ÖZHAN

YEDEK ÜYE

Doç. Dr. Gülistan Meşe ÖZÇİVİCİ

TABLE OF CONTENTS

LIST OF TABLES

LIST OF FIGURES

ABBREVIATIONS

2-HG: 2-Hydroxyglutarate

3C: Chromosome Conformation Capture

4C: Circular Chromosome Conformation Capture

CCDC26: Coiled-coil domain containing protein 26

CGI: CpG Island

CNS: Central Nervous System

CpG: 5'-C-phosphate-G-3'

Dox: Doxycycline

GBMs: Glioblastomas

G-CIMP: Glioma CpG island methylator phenotype

GWA: Genome-wide Association

HIF1A: Hypoxia inducible factor 1

IDH: Isocitrate Dehydrogenase

IHA: Immortalized Human Astrocytes

IPSC: Induced Pluripotent Stem Cells

NHA: Normal Human Astrocytes

PHD: Prolyl Hydroxylase

PI3K: Phosphoinositide 3- Kinase

TET2: tet methylcytosine dioxygenase 2

WHO: World Health Organization

α-KG: Alpha- ketoglutarate

ACKNOWLEDGEMENTS

First, I would like to express my special thanks to my advisor Dr. Yavuz OKTAY. I have always been motivated by his knowledge, experience and understanding in my work.

After that, I would like to thank my lab mates Burcu EKİNCİ, Ece SÖNMEZLER, Aykut KURUOĞLU, Kaan OKAY, Fadime ÖZTOPRAK and Ebru DİLER who are always supportive and brother-in kind in the laboratory. However, I want to make my special thanks to Burcu, she taught me everything she knew from the first day I came to the laboratory three years ago, and we learned a lot together and we shared and collected endless moments while becoming very good friends.

Besides my own laboratory, I would like to thank Uğur TÜFEKÇİ and Soheil AKBARİ for unlimited help about my works and their understanding. I would also like to thank my friends, Tülay KARAKULAK, Merve TÜRKER, Betül TERCAN, Melike TETİK OKTAY, Cumhur DOĞAN, Murat GÜNGÖR, Aslı TİMURBOĞA and Gökçe SENGER who never leave me alone with their friendship, and who always have moral support when writing my thesis. And I want to thank Negüzel ŞAHİN to become my second mother in IBG.

I would like to thank my dear friend Engin TATLIDİL, who motivated each other with coffee for not giving up. In addition, I would also like to thank my friend Bleda OĞUZ who helped me organize my thesis with his English knowledge.

Last but not least, I would like to thank my family, my parents Esra YARAŞ and Sedat YARAŞ, who always support me financially and spiritually and thank my brother Oğulcan and sister Sıla for being in my life. Finally, I would like to thank İzel MERCAN for having endured all my moods during my thesis and always with his love and support.

June 2019 Tutku YARAŞ

INVESTIGATION OF CHROMATIN-CHROMATIN INTERACTION OF GLIOMA RISK LOCUS AT 8q24.21 by CHROMOSOME CONFORMATION CAPTURE TECHNIQUES AND EFFECTS OF IDH MUTATIONS

Tutku YARAŞ, Dokuz Eylul University Izmir International Biomedicine and Genome Institute, tutku.yaras@msfr.ibg.edu.tr

ABSTRACT

Brain tumors are poorly diagnosed and cause to death of thousands of people around the world every year. Gliomas are the most common brain tumors. Although there have been many mutations associated with gliomas to date, IDH (Isocitrate Dehydrogenase) mutations have been identified as “driver mutations” and are seen in about 80 percent of cases. The number of mutations associated with gliomas has increased day by day. GWAS (Genome Wide Association Studies) has identified significant risk locis and important steps have taken to diagnosis of the disease. The aim of this project is to identify at the molecular level of the mechanism of action of the single nucleotide polymorphism (SNP) rs55705857 G allele,which was found by GWAS, which is located in the 8q24.21 region and is defined as the mostly related glioma allele, and demonstrates its association with the IDH1-R132H mutation. For this purpose, interactions with the risk allele in the immortalized human astrocyte (IHA) cells with and without IDH1-R132H mutation were identified and the candidate interactions that increase the susceptibility to gliomagenesis were determined. In addition, the risk allele was created in the IPSCs (Induced Pluripotent Stem Cells) by genome regulation and increase in the expression of MYC was observed. In addition, expression of MYC has also been found in 2-HG (2-hydroxyglutarate, oncometabolite of IDH-R132H mutations) treated IHA-R132H cells. Our results show that rs55705857 regulates expression of the MYC gene through long-range chromatin-chromatin interactions. The increase of MYC expression due to IDH1-R132H mutation / 2-HG may explain the 8q24-associated glioma risk being specific to IDH-mutant tumors. In conclusion, understanding the mechanism of glioma susceptibility sheds light on the early stages of tumor formation.

Key words: Glioma, IDH-R132H, 4C-seq, 8q24.21

KROMOZOM KONFORMASYONU YAKALAMA TEKNİKLERİYLE 8q24.21 BÖLGESİNDEKİ GLİOMA RİSK-LOKUS ALANLARININ KROMATİN-KROMATİN ETKİLEŞİMLERİNİN BELİRLENMESİ VE IDH MUTASYONUNUN ETKİSİNİN ARAŞTIRILMASI

Tutku YARAŞ, Dokuz Eylül Üniversitesi İzmir Uluslararası Biyotıp ve Genom Enstitüsü,

tutku.yaras@msfr.ibg.edu.tr

ÖZET

Beyin tümörleri zayıf teşhisi olan ve her yıl dünyada binlerce insanın ölümüne neden olan vakalardır. Beyin tümörleri arasında en yaygın olarak görülenler gliomalardır. Bugüne kadar, gliomalarla ilişkilendirilen pek çok mutasyon olmasına ragmen IDH (İzositrat Dehidrojenaz) mutasyonları "sürücü mutasyon" olarak tanımlanmış ve vakaların yaklaşık yüzde 80 inde görülmektedir. Yapılan çalışmalarla gliomalarla ilişkilendirilen mutasyonların sayısı gün geçtikçe artmıştır. GWAS (Genom Boyu İlişkilendirme Çalışmaları) ile önemli risk lokusları tanımlanarak hastalığın tanısı için önemli adımlar atılmıştır. Bu projenin amacı GWAS çalışmalarında tanımlanan 8q24.21 risk bölgesinde konumlanan ve en güçlü yatkınlık aleli olarak gösterilen tek nükleotit varyantı (SNP) rs55705857 G alelinin moleküler seviyedeki etki mekanizmasını anlamak ve IDH1-R132H mutasyonuyla olan ilişkisini ortaya koymaktır.Bu amaçla, IDH1-R132H mutasyonu içeren ve içermeyen ölümsüzleştirlmiş insan astrosit hücrelerinde (IHA) kromozom konformasyonu yakalama yöntemleriyle, risk aleliyle olan etkileşimler belirlenerek gliomagenez sürecini tetikleyen aday etkileşimler belirlenmiştir. Ayrıca, risk aleli genom düzenleme yöntemi ile uyarılabilen pluripotent kök hücrelerde oluşturulmuş ve MYC ifadesinde artış gözlenmiştir. Ek olarak, MYC ifadesi 2-HG (2-hidroksiglutarat, IDH-R132H ın onkometaboliti olarak bilinmekte, ile muamele edilen R132H mutasyonu içeren ölümsüzleştirilmiş insan astosit hücrelerinde de görülmüştür. Elde ettiğimiz sonuçlar, rs55705857'nin uzak mesafeli kromatin-kromatin etkileşimleri sayesinde MYC geninin ifadesini düzenlediğini göstermiştir. IDH1- R132H mutasyonu/ 2-hidroksiglutarata (2-HG) bağlı MYC ifadesinin artması, 8q24 ilişkili gliom riskinin IDH-mutant tümörlere özgü olmasını açıklayabilir. Sonuç olarak, glioma yatkınlığının mekanizmasının anlaşılması, tümör oluşumunun erken evrelerine ışık tutar. Bulunan yeni etkileşimler de hastalığın tedavi ve tanısında yeni olanaklar sağlayabilecektir.

Anahtar Kelimeler : Glioma, IDH-R132H, 4C-seq, 8q24.21

1 INTRODUCTION AND AIM

Glioma is a type of tumor that occurs in the brain and spinal cord. It is known that brain tumors are complex diseases, there are too many risk factors, and acting mechanisms of most of the risk factors have not been known yet. Diffuse gliomas develop due to molecular and genetic alterations that further accumulate with tumor progression. IDHI & IDH2 mutations are the one of the most critical for glioma formation and 70-80% of IDHI & IDH2 mutations were identified in diffuse grade II & III gliomas. Further studies have shown that IDH mutations are early events in gliomagenesis as driver mutation (Parsons et al., 2008). Recent studies have shown that the rs55705857 SNP region at 8q24.21 is highly related to glioma subtypes and is assigned to increase the risk of glioma formation risk more than 5 times for all gliomas and 10 times more risk of IDH mutated gliomas. Other evidence was about that the region encompassing rs55705857 may act as a MYC enhancer (Oktay et al., 2016) For these reasons, it is important to demonstrate rs55705857 and IDH mutation relation at molecular level and SNP's effects on gliomagenesis.

1.1 Aim of the Study

The purpose of this project is to explain mode of action of 8q24.21 region and SNP rs55705857, determined by GWA studies, to light up early stages of gliomagenesis Therefore, we hypothesize the understanding of IDH1 R132H mutation and rs55705857 G allele relationship and their acting mechanism at molecular level. To achieve this, firstly, 4C-Seq was used to illuminate the possible mechanism of action of SNP rs55705857 for gliomagenesis by using IDH-wt and IDH1-R132H immortalized human astrocytes.

2 GENERAL INFORMATION

Brain tumors have poor prognosis, higher morbidity and mortality, although they are rare according to other tumors (González-Castro et al., 2019). Every year, in the US 18000 and in Europe 26000 new cases is occurring and in US 13000 deaths are recorded because of primary brain tumors and CNS tumors (Kinnersley, Houlston, & Bondy, 2018; Louis et al., 2016). However, these tumors cannot be diagnosed clearly. So they are rather important health problem for humanity (González-Castro et al., 2019). Understanding the early stages of gliomagenesis and epigenetic interactions construct hypothesis of this study.

2.1 Gliomas

The term glioma is used for tumors that come from glial cells and their surrounding supporting neurons. This term also includes astrocytic tumors (González-Castro et al., 2019). The most common type of fatal brain tumors is glioma, which forms 80 % of all brain tumors (González-Castro et al., 2019). Gliomas are classified by the WHO Classification in 2016 based on histopathological and clinical criteria that categorized gliomas from grade I to IV as shown in **Table 2.1** (Yan et al., 2009).

Table 2.1: Table shows widespread features and some examples for 2016 WHO CNS tumor Classification (Tateishi & Yamamoto, 2019; Yan et al., 2009).

WHO GRADES	COMMON FEATURES & EXAMPLES
WHO Grade I	➢ Benign mostly ➢ Often curable by surgical intervention ➢ Rarely turn into high grade lesions
WHO Grade II & III	➢ Malignant and invasive mostly ➢ Often turn into high grade lesions Example: Diffuse astrocytomas (Grade II, IDH mutant, wt or NOS), Oligodendrogliomas (Grade II), Anaplasmic Oligodendrogliomas (Grade III) (IDH mutant, 1p/19q codeletion or NOS(Not Otherwise Specified))
WHO Grade IV	➢ Mostly invasive ➢ Poorly prognoses ➢ Mostly malignant Example: Glioblastoma (IDH mutant, wt or NOS)

2.1.1 2016 WHO Classification of Gliomas

In the past century, CNS tumors classification is only dependent on histological parameters by observing light microscopy through hematoxylin- eosin staining (Louis et al., 2016), but it is distinct for categorization and prognosis due to the surgical complexity of tumor sampling and limited number of samples have led to misprognosis for diffuse gliomas. Therefore, finding molecular markers correctly, not only important for classification of CNS tumors, but also other types of cancer for prognosis and treatment (Iorgulescu et al., 2019).

Understanding of mechanism of gliomagenesis and finding out new biological markers has made it easy to reinforce classification and finding new therapeutic targets. In the last 20 years, molecular studies have been carried out in order to understand the tumor formation more clearly (Louis et al., 2016). These studies and found markers, such as IDH mutation, 1p/19q codeletion, loss of expression in ATRX gene, mutation in TERT, H3-K27M mutations that have made the 2016 WHO classification more precise, based on molecular classification as shown in **Figure 2.1** 2016 WHO associates genotypic and phenotypic parameters to classify tumors of CNS (Reifenberger, Wirsching, Knobbe-Thomsen, & Weller, 2016).

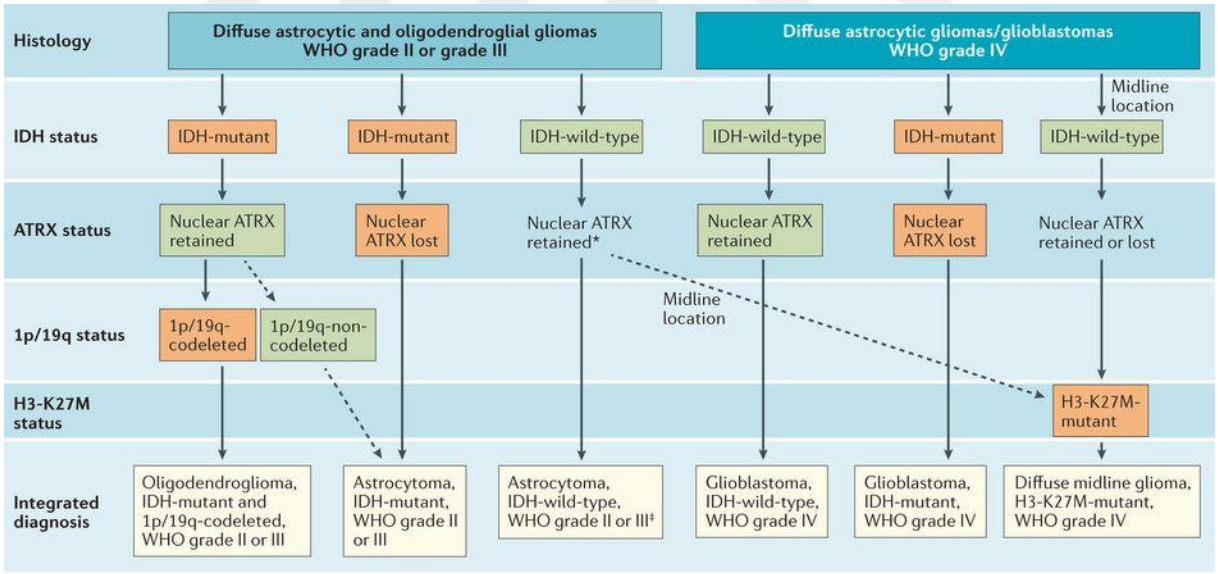

Figure 2.1: Available molecular and histological markers to categorize diffuse gliomas according to 2016 WHO Classification. Classification of diffuse gliomas are primarily based on IDH mutation status. After that, ATRX expression and 1p/19q codeletion as well as H3-K2M mutations are considered for their grade determination and classification (Reifenberger et al., 2016).

In 2016 WHO, these new, narrower definitions, allow for more homogeneous definitions, while more accurate and definitive judgments can be reached made in the diagnosis enabling more accurate treatment methods. Considering all this together, it can be said that the 2016 WHO classification have been facilitating clinical, experimental and epidemiological studies and guides the development and improvement of the lives of people living with brain tumors (Louis et al., 2016).

2.1.2 Nomenclature and Identification of Gliomas

CNS tumor diagnoses were executed by separating the histopathological names with a comma and following the genetic characteristics and adjectives according to the 2016 WHO CNS Classification. In this nomenclature, when special gene names are written in Italic, gene families are typically written and roman numerals indicate the grades of WHO. Glioma name and part of the definition are written in Italic. After that, other properties that are characteristic but not necessary for diagnosis are usually written typically and definition is completed. For instance, Oligodendrogliomas have been named and defined as *Oligodendroglioma,* IDH-*mutant* and *1p/19q co-deleted,* "Microcalsicifitions are typical" (Louis et al., 2016).

Table 2.2: Table shows known mutations related to nucleotide and amino acid changes in IDH1 and IDH2 (Madala et al., 2018).

Gene	Nucleotide Change	Aminoacid
IDH1	**G395A** C394T C394G C394A G395T G299A	**R132H** R132C R132G R132S R132L R100Q
IDH2	**G515A** G515T A514T G516C G419A G419T C418T C418G	**R172K** R172M R172W R172S R140Q R140L R140W R140G

2.1.3 IDH Mutations in Gliomas

IDH is a cytosolic NADP or NAD dependent protein, which is located at region 2q34 which is known as most protected region of chromosome. α-KG is formed by decarboxylation of isocitrate and this reaction is catalyzed by IDH. Three isozymes of IDH exist as IDH1, IDH2 and IDH3 and they are encoded by 5 different genes (Cohen, Holmen, & Colman, 2013). Mainly, all of them catalyze isocitrate but their cofactor is used location in cell, metabolism in which they take place can show some differences as shown in **Figure 2.2.** (Ichimura, 2012).

The discovery of IDH1 mutation in gliomas has clearly been a milestone in neuro-oncology in recent years, firstly IDH mutations were found in colorectal cancers through sequencing techniques (Yen, Bittinger, Su, & Fantin, 2010). After that 22 glioblastoma samples were analyzed by whole-exome sequencing and these mutations were first discovered in 2008 (Cohen et al., 2013; Parsons et al., 2008). According to ongoing studies, IDH mutation was defined as "driver mutation", which is found in 90 percent of cases, so, it is quite important mutation for low-grade diffuse gliomas and secondary glioblastomas (Iorgulescu et al., 2019; Tateishi&Yamamoto,2019).

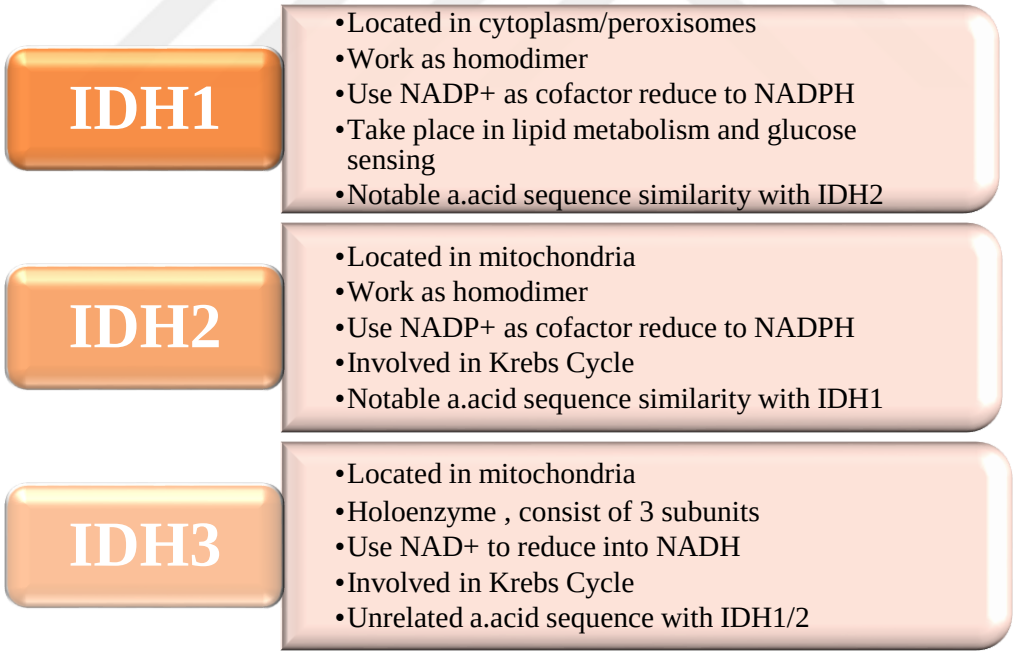

Figure 2.2: Similarities and differences among three isozymes of IDH. Although there are some differences, all isozymes are used to catalyze isocitrate decarboxylation to produce α-KG, which take place in different sub-pathways in cell metabolism (Ichimura, 2012; Tateishi & Yamamoto, 2019).

To catalyze isocitrate, homodimer of IDH1 binds to active closed conformation. Although, plenty of amino acid residues are present in the binding site, only R132 makes three hydrogen bonds, making it a preferential target for glioma mutation (S. Zhao et al., 2009). If substitution occurs at R132 codon, this can result in weakening binding of isocitrate. R172 codon in IDH2 corresponds to R132 with IDH1, they are analogous regions. The reason why mutations in IDH1/2 only target these amino acids can be explained by the following physicochemical factors (Ichimura, 2012).

Research has shown that all IDH1 and IDH2 missense mutations. These mutations happen at codon 132 and histidine amino acid is formed instead of arginine, which can be demonstrated by immunohistochemistry staining, because at this codon second nucleotide is transited from G to A (Ichimura, 2012; Iorgulescu et al., 2019). Of course, uncommon types of IDH1/2 mutations have been found as shown in **Table 2.2**, but these mutations of R132 and R172 are very common for gliomas (Ichimura, 2012).

2.1.3.1 Consequences of IDH Mutation in Gliomas

Mutations in IDH gene occur at early stages of gliomagenesis and enzyme function changed, it did not produce NADPH by reducing NADP+ and 2-HG is produced instead of α-KG (Cohen et al., 2013). In this type of mutation, mutation generally occurs at single copy of the gene in tumors. As a result, such a mutation is not just about the loss of function but the gain of neomorphic enzymatic activity (Ichimura, 2012; Yen et al., 2010). When arginine turns to histidine at codon 132. Structural research indicates that, active site of IDH1 residue is shifted as shown in **Figure 2.3**. These residues are shifted to generate stable structural changes to reduce isocitrate and obtaining 2-HG instead of α- KG (Dang et al., 2009). In the beginning, according to the *in vivo* studies, how IDH mutations support oncogenic transformation was ambiguous. Then, *in-vitro* research has shown us that IDH mutations are always heterozygous mutations. So both mutant and wt IDH alleles are needed to produce 2-HG. When comparing IDH-mutant cells with IDH-wt cells, it is clear that the 2-HG level is 50-100 times greater than that of IDH-wt cells (Dang et al., 2009; Ward et al., 2010). These indicates help in hypothesizing that mutant IDH could be an oncogene and its product 2-HG could be an "oncometabolite" (Cohen et al., 2013). Currently, formed 2-HG is known as oncometabolite and it can cause epigenetic changes that can accelerate tumor formation. Therefore, understanding the biological role and other correlations of this mutation in gliomagenesis will be a quite important approach for future therapies (Tateishi & Yamamoto, 2019).

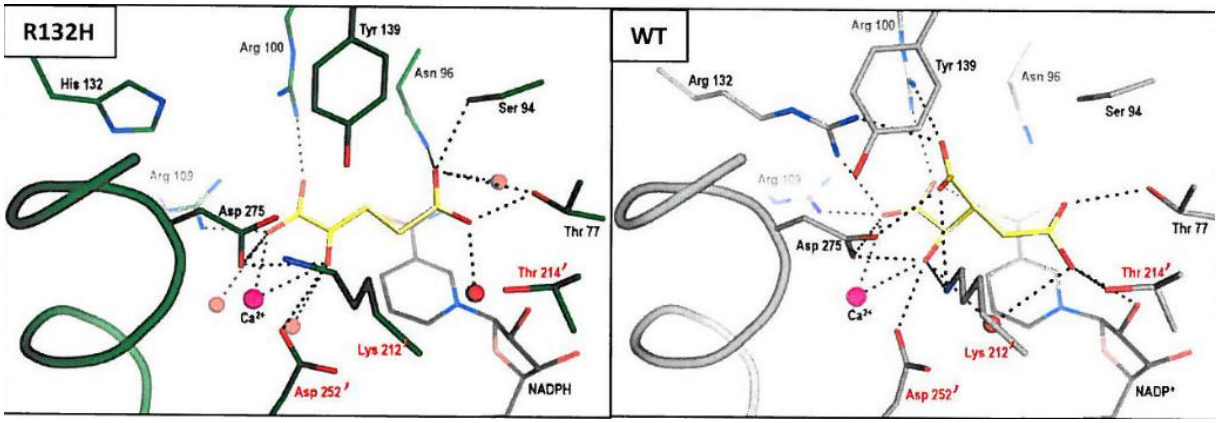

Figure 2.3: Comparison of IDH R132H and wt IDH proteins. In these figures at the left, yellow part refers to α-KG; gray refers to NADPH for R132H mutant type of IDH's active site. At the right part, active site of wt IDH1 is demonstrated and when yellow part indicates to isocitrate, gray part indicates to NADP (Dang et al., 2009).

2.1.3.2 Cellular Functions of IDH Mutation and 2-HG

Before mutations at R132 and R172 were observed, no interaction of IDH genes with cancer were established. However, research has indicated that IDH mutations take role in different types of tumor such as leukemia, T-cell lymphoma, prostate cancer, AML (Acute Myeloid Leukemia) and so on. IDH takes place in different metabolisms of cells and also has an effective role in the citric acid cycle, which shows that it is an important component of cell protection against oxidative stress (Cohen et al., 2013).

In addition, it is well known fact that the HIF1A activity is affected by IDH mutations. Since in the presence of 2-HG, HIF1A cannot be hydroxylated and could not be recognized by proteasome and is upregulated and effect transcription of different genes that play a role in pyruvate metabolism, ATP synthesis, mTOR signal pathway, glutamate metabolism, and so on (Dang et al., 2009).

Until now, only two studies have shown molecular and genetic tumor markers by analyzing huge numbers of glioma samples. According to these studies, different markers are presented, but only TP53 mutation and increasing EGFR are common among these studies. Aforementioned markers were accepted as IDH-mutant gliomas' molecular pathology markers (Schwartzbaum, Fisher, Aldape, & Wrensch, 2006).

All of such markers can cause cell proliferation and cell metabolism to change. In addition, recent studies have shown that tumorigenesis and malignancy in IDH mutant gliomas

are related to PI3K pathway and activation of MYC. So, it can be said that the mutation of IDH induces gliomagenesis through tertiary mutations and epigenetic changes (Tateishi & Yamamoto, 2019).

2.1.3.3 Epigenetic Modifications in IDH Mutant Gliomas

The human DNA sequence consisting of three million base pairs in the nucleus inside the cell is organized in the form of chromatin structure. Chromatins consist of repetitive regions called nucleosomes, formed by eight histone proteins that are chemically modified by methylation or acetylation. DNA methylation, histone modifications, nucleosome remodeling, small and long non-coding RNAs and DNA- protein interactions change three-dimensional chromatin structure (Malta et al., 2017).

In the meaning of DNA methylation is that methyl group is covalently transferred to 5' of cytosine ring and it essentially occurs at CpGs, 5-mC is formed at the end of the methylation process. DNMT (DNA methyl transferase) enzymes are responsible for methylation and TET1/2 enzymes are responsible for 5-mC demethylation (Malta et al., 2017). IDH mutations have been associated with CpG-island hypermethylation, CpG hypermethylation is observed in the tumor suppressor genes' promoter region (Madala et al., 2018). In addition, in spite of IDH mutant glioma samples are related with DNA hypermethylation, no TET mutation was found in glioma samples. This is due to the fact that α-KG dependent enzymes cannot function properly due to mutation (Lu et al., 2012). Although 2-HG is similar to α-KG as structurally, 2-HG inhibits some dioxygenases and histone demethylases such as TET2 and KDM (JmjC domain bearing histone demethylases) improperly (Madala et al., 2018). Additionally, in IDH mutant gliomas, highly methylated MGMT (O-6-methylguanine DNA methyl transferase) promoters are observed, which is related with DNA repairing pathway (Tateishi & Yamamoto, 2019).

TET2 is inhibited due to 2-HG and DNA methylation has begun and this situation can form special methylation patterns for tumor cells such as G-CIMP (Tateishi & Yamamoto, 2019). Turcan et al. article showed this situation through IDH mutated NHA cells and after a while G-CIMP positive GBMs were formed as expected (Turcan et al., 2012). Additionally, these NHA cells with IDH mutation have an increase in H3K9me3 (trimethylation of histone 3 lysine 9) level, which could be observed before DNA methylation changes (Lu et al., 2012), this event suggests that histone methylation could be an earlier effect in tumors with IDH

mutation, so if prognosis could be done correctly, imprinted cell differentiation because of this methylation can be fixed by correct therapies (Rohle et al., 2013; Turcan et al., 2013).

In addition, CpG rich intergenic regions may include enhancer, silencer and insulator, which are distal genomic regulatory elements. Those have DNA-binding transcription factors recognition sites. Transcription can be enhanced or repressed in this way. As mentioned above, the interaction between protein and DNA determines the spatial organization of the genome and because of these interactions, chromatin loops are formed by insulator protein. CTCF (CCCTC-binding factor) is one of important insulator protein, which takes important role in stabilization of enhancer-gene interaction in intergenic regions. However, CTCF binding weakens by hypermethylation in IDH mutant gliomas, so enhancer-gene interactions cannot be protected and oncogenic pathways are regulated (Malta et al., 2017). **Figure 2.4** indicates main results of IDH mutation in LGG cell (Madala et al., 2018). When all considered, understanding the changes in three-dimensional chromatin structure and epigenetic arrangements are important in terms of understanding the gliomagenesis process, prognosis and possible therapeutic pathways.

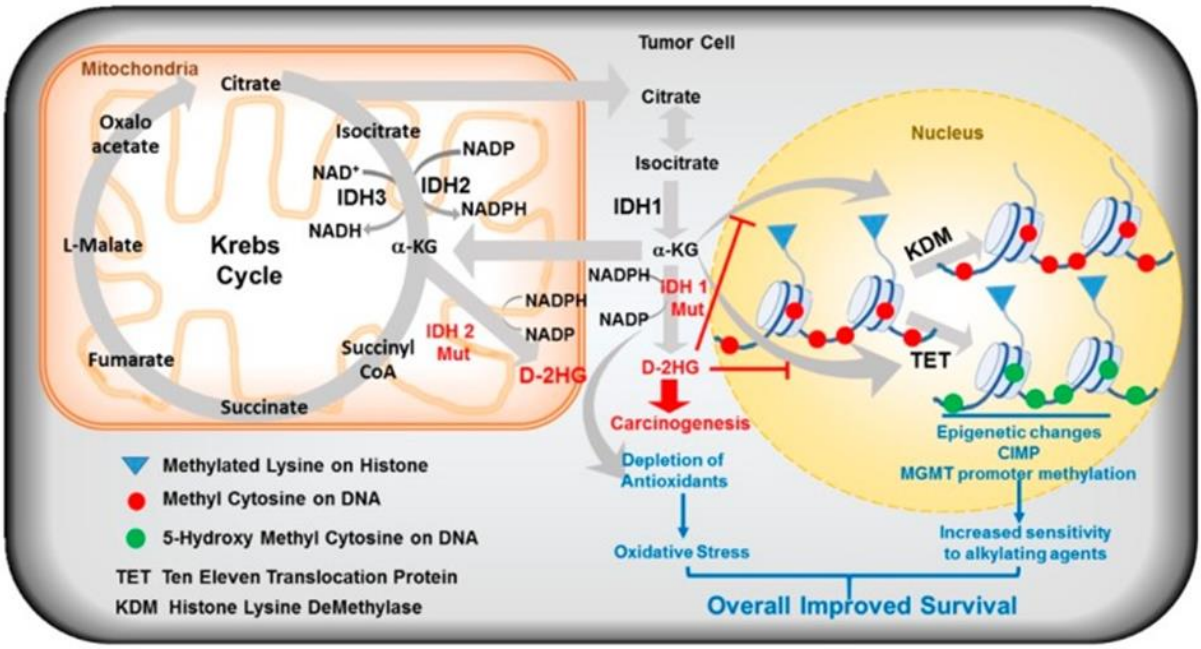

Figure 2.4: Demonstration of main alterations in IDH mutant glioma cells. In the presence of 2-HG because of enzyme activation or inactivation epigenetic alterations occur and cellular pathways are changed through gliomagenesis (Madala et al., 2018).

2.1.4 Determined Variants in Gliomas by GWA Studies

Gliomas are one of the most aggressive but least understood tumors affecting people. Although genetic inheritance affects the risk of glioma formation, most of the risk factors have not been determined. Therefore, the genetic role of polymorphisms, which are genetic variants in the genome, has been tried to be determined, but they are still largely unknown (González-Castro et al., 2019). For these reasons, ongoing studies will provide new perspectives for gliomas and will also provide clinically advantages (Rajaraman et al., 2012).

Table 2.3: List of important GWA studies on gliomas and found risk regions.

Year of GWAS	Research Groups	Used populations/Numbers	Identified risk loci's
2009	Shete and colleagues (Shete et al., 2009)	UK & European-American Individuals 1878 cases-3670 controls	5p15.33 8q24.21 9p21.3 11q23.3 20q13.33
2011	Sanson and colleagues (Sanson et al., 2011)	UK & European-American Individuals 4147 cases- 7435 controls	7p11.2
2014	Walsh and colleagues (Walsh et al., 2014)	UK & European-American Individuals 1013 cases- 6595 controls	3q26.2 7p13.1
2017	Melin and colleagues (Melin et al., 2017)	Meta-analysis of existing GWAS and 2 new GWAS 12496 cases – 18190 controls	5 for GBMs; 1p31.3 11q14.16 16p13.3 16q12.1 22q13.1 8 for non GBMs; 1q32.1 1q44 2q33.3 3p14.1 10q24.33 11q21 14q12 16p13.3

Human genome project was completed in the year 2000, which allowed genetic variants to be identified in the genome. This was important for cancers especially for gliomas. Following this project, analytical platforms have been developed that provides to maintain Genome Wide Association Studies (GWAS) at low cost (Liu et al., 2010). GWA studies provide to determine new genes or single nucleotide polymorphisms (SNPs) that are related with diseases. SNPs are included in at least 1 % of populations and these variants can affect structure of gene product or function, so, when they combined with other changes in the genome, they can cause individual differences in disease formation (Schwartzbaum et al., 2006). In these studies, two groups are compared, cases and controls groups, and attempted to discover new variants associated with loci and traits related to specific diseases or cancers (Kinnersley et al., 2018).

GWA studies on the determination of germline variants associated with glioma susceptibility were conducted and the first successful report was published in 2009. These studies have shown that, risk of glioma formation is increased by low penetrance susceptibility alleles that can light up the formation of primary brain tumors (Shete et al., 2009). Until now different GWA studies have been performed and in total 25 polymorphism loci have determined related to glioma susceptibility, as shown in **Table 2.3.**

2.1.4.1 Rs55705857 at 8q24.21 loci associated with glioma susceptibility

It has been shown that 8q24.21 region causes an increase in glioma formation (Enciso-Mora et al., 2013). Determined risk region is located in gene desert area as shown in **Figure 2.6,** but it is related to the different cancer types and it is known as pleiotropic cancer locus (Kinnersley et al., 2018). Most known cancer related genes are nearly 1,5 Mb far away from this region, which can hypothesize the synthetic association or long-range disequilibrium (LD) with this region (Jenkins et al., 2012). This locus also includes oncogene MYC, and alterations in this region may affect MYC activity (Kinnersley et al., 2018).

Detailed studies (GWA and candidate gene studies) have demonstrated that the coiled-coil domain containing protein 26 (CCDC26) is located at 8q24.21 region and it is related to low-grade glioma formation(González-Castro et al., 2019). The CCDC26 region plays role in the regulation of retinoic acid that phosphorylate c-AMP responsive element binding protein and, which stimulates caspase 8 transcription in apoptosis. (Shete et al., 2009; Simon et al., 2010). Continuing studies have shown that, telomerase activity is downregulated in

neuroblastoma and GBM cell by CCDC26 gene activity, which can lead to increased apoptosis(González-Castro et al., 2019).

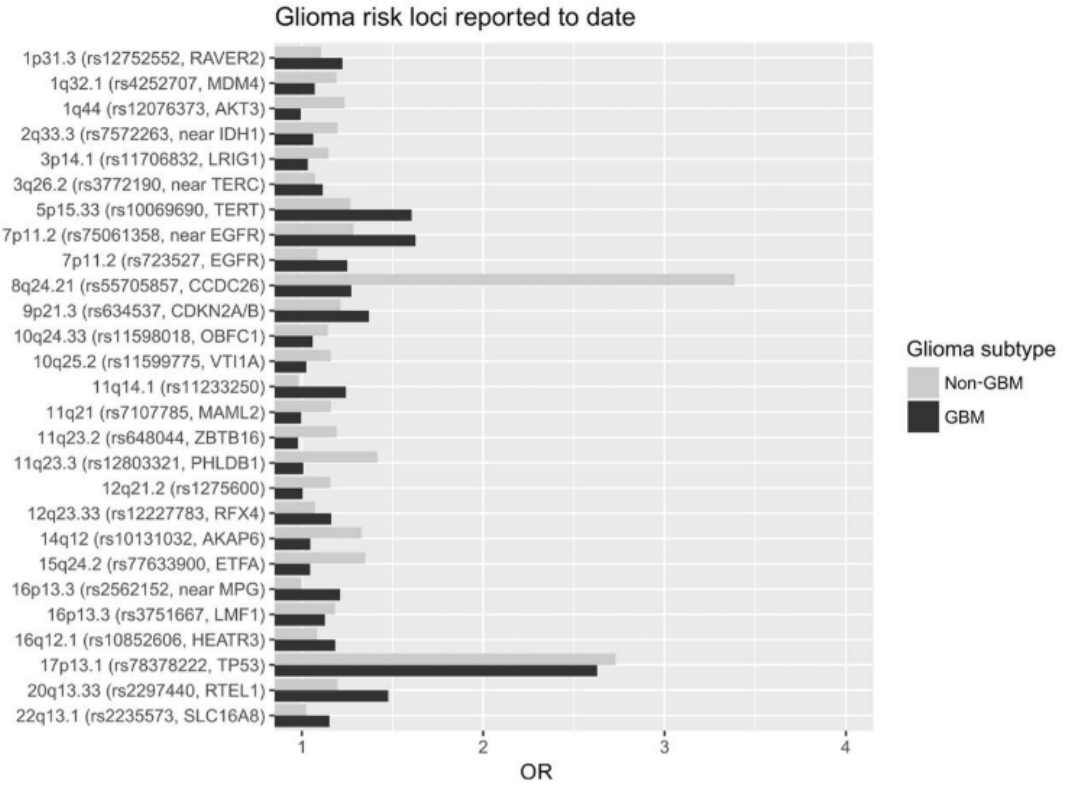

Figure 2.5: It shows identified risk loci and odds ratios by GWAS. Determined risk alleles and their relative impacts were shown for GBM and non-GBM cases so far. The highest odds ratio belongs to Rs55705857 allele for non GBM cases (Rajaraman et al., 2012).

After 8q24.21 region has been shown to be related to gliomagenesis, importance of CCDC26 for glioma susceptibility, SNP genotyping, long range PCR and NGS analysis have been performed, and some variants have been found as candidate alleles such as rs891835, rs6470745 and rs55705857 (González-Castro et al., 2019; Jenkins et al., 2012; Oktay et al., 2016). However, rs55705857 have been defined as causative allele at first time by Jenkins group and mechanism of allele have not been reported (Jenkins et al., 2012). After that, it has been determined as the most strongly associated allele as shown in **Figure 2.5** and then its odds ratio have found nearly six for subtypes of oligodendrogliomas (Oktay et al., 2016). Previous studies in our laboratory have shown that this SNP increases glioma susceptibility, especially when there is IDH mutation, but SNP does not significantly affect glioma susceptibility when IDH is wt. All in, rs55705857 shows the strongest effect in low-grade gliomas,

oligodendrogliomas and astrocytomas due to IDH mutation. Although, it is assumed that IDH-mutant -MYC or SNP-MYC functional interactions exists , clear mechanism has not been reported (Oktay et al., 2016). It has been also shown that existing both rs55705857 and IDH mutations can increase glioma formation by 8-10 times (Enciso-Mora et al., 2013)

As shown in **Figure 2.6**, rs55705857 is located at conserved region of CCDC26, which is estimated as long non-coding RNA (lncRNA). The area of this SNP is (15bp area) 100% conserved from platypus to human. This conserved region is located in an unmethylated CpG cluster. (Jenkins et al., 2012). In our laboratory, previous studies have shown that when IDH is mutant rs55705857 risk allele increase glioma risk comparing to IDH wt (Oktay et al., 2016). According to these studies, it is assumed that IDH R132H–MYC or SNP-MYC functional interactions can be formed, but clear mechanism has not been reported. Additionally, previous studies of Oktay Group have shown that rs55705758 risk allele may act as MYC enhancer by using Luciferase Reporter Assay. However, results shows interactions of risk allele and IDH mutations indirectly (Oktay et al., 2016).

Considering these, it can be predicted the importance of this conserved area, but it should be clear that the mechanism of action of the region. Although many glioma risk alleles have been identified so far, their molecular mechanism has not yet been fully elucidated (Kinnersley et al., 2018).

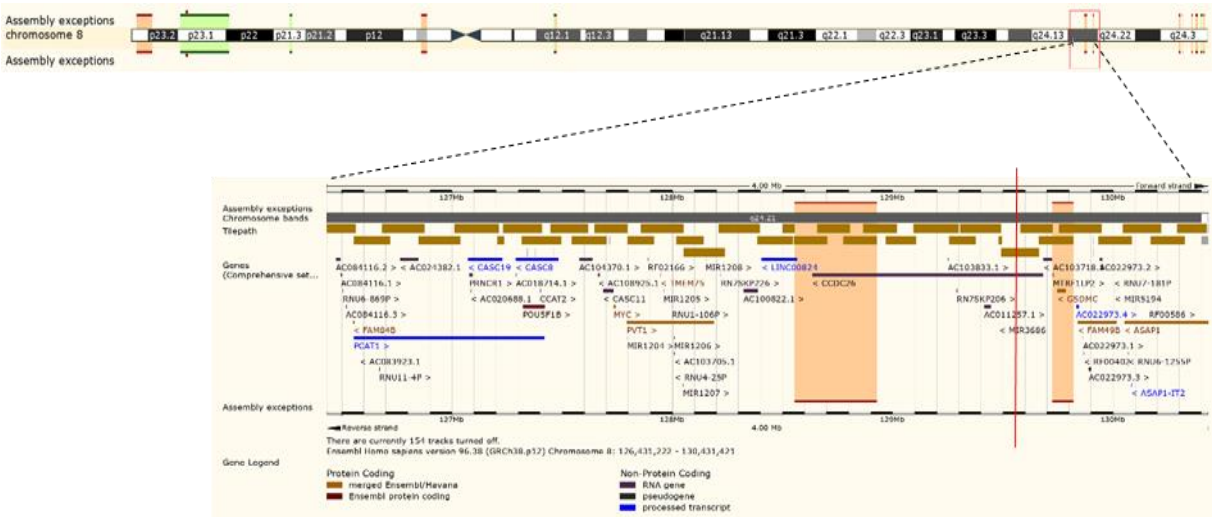

Figure 2.6: It shows chromosome 8 and 8q24.21 region. Figure was taken from Ensembl Human GRCh38.p12 library (vertical red line indicates rs55705857 allele location).

2.2 Development of Chromosome Conformation Capture Methodologies

Major chromosome activity depends on both the structural and spatial conformations of genome. Chromatin loops, inter-chromosomal interactions are important for gene expression and recombination. In higher eukaryotes, transcription is controlled by regulatory elements, such as enhancer, insulator, which can be recognized by transcription factors. They also play role in formation of three-dimensional chromatin loops .In many cases, regulatory elements can be located a few Mb away from the target gene, they do not have to be close to the target genes. They can be in trans-interaction. All these chromosomal organizations are dynamic and can vary by cell cycle or cell type. For those reasons, functional connectivity and interactions of genes and regulatory elements should be mapped to understand complex network genome interactions (Dekker, 2006; Dekker, Rippe, Dekker, & Kleckner, 2002a). Microscope or FISH techniques have some limitations in determining chromosome conformations. Therefore, Dekker and colleagues have improved the high-throughput technique to determine spatial organization of chromosome. This technique was called as "Chromosome Conformation Capture", "3C". 3C provides to assign interactions between two genomic loci. It can be applied from bacteria to humans (Dekker, Rippe, Dekker, & Kleckner, 2002b). In basic logic, chromatins are fixed by formaldehyde, then restricted by restriction enzymes and ligation is performed, formed DNA pieces are analyzed. In this way, 3C provides for the determination of one to one interactions in three-dimensional chromatin structure (Dekker et al., 2002b).

Nowadays, 3C technique has become more common, it has been used as routine technique, and then new techniques have been developed with same logic but they have been developed to determine more specifically the spatial organization of the genome (Gavrilov et al., 2009). 3C can explain interactions between known regions, but it cannot explain interactions between unknown regions. Therefore, "4C", "Circular Chromosome Conformation Capture" techniques were first developed (Z. Zhao et al., 2006). In this approach, there are additional steps; circularization, PCR amplification of ligation products and high-throughput screening by microarray. After that, 4C , 5C, Hi-C and CHIA-PET technologies have been developed as shown in **Figure 2.7** (Sati & Cavalli, 2016)**.**

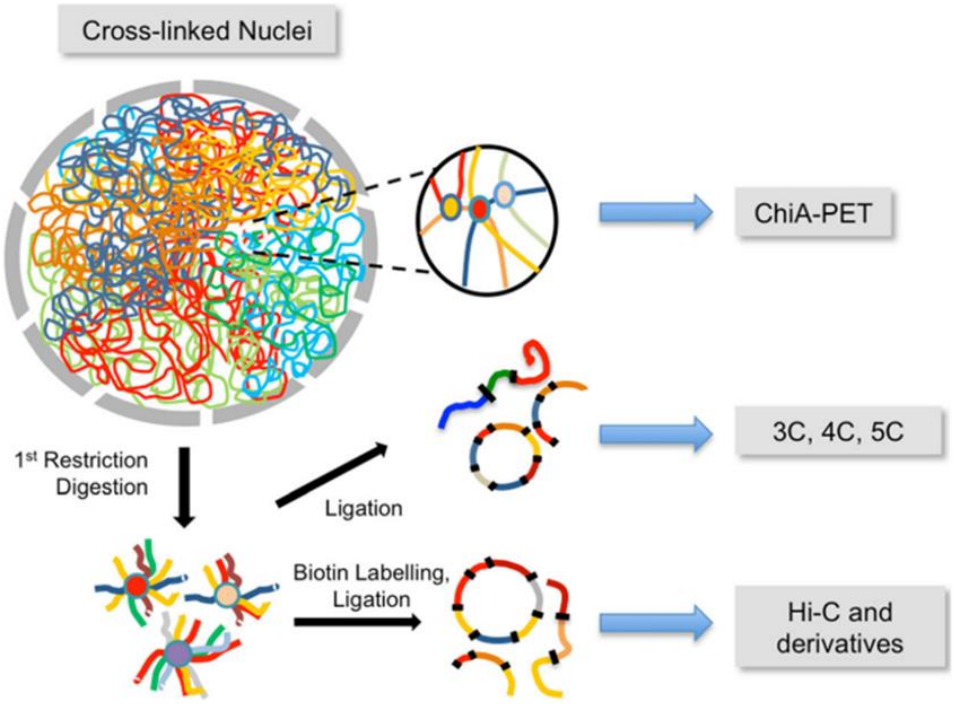

Figure 2.7: It demonstrates chromosome conformation capture techniques. 3C derived techniques are based on formaldehyde cross-linking of nuclei, then restriction, ligation, amplification steps are followed and all is analyzed in different ways. ChiA-PET combines Hi-C technology with Combining Protein Immunoprecipitation (ChIP-Seq) techniques. Hi-C derivative techniques combine biotin labeling and classical 3C logic (Sati & Cavalli, 2017)

2.2.1 One to all approach: Circular Chromosome Conformation Capture and Sequencing (4C-Seq)

4C- Sequencing technology is derived from 4C methods adapted to 3C.The difference is that when 4C technology uses microarray to analyze samples, 4C- Sequencing technology uses Illumina sequencing technologies. 4C methods use one to all principle instead of one to one principle of 3C. Single genomic region is chosen and called as "view point or bait". The aim of this method is to determine of the relationship between view point and the entire genome These interactions can be cis (on the same chromosome) or trans (on other chromosome) (Grob & Cavalli, 2018; Matelot & Noordermeer, 2016). The general 3C technique is applied to prepare 4C-Seq library, but 4C have secondary restriction and ligation process. After that, DNA samples become ready for the amplification process. Designed primers are used according to inverse PCR to amplify interacting region and purified PCR samples are sequenced by Illumina NGS technology as shown in **Figure 2.8** (Van De Werken et al., 2012)**.**

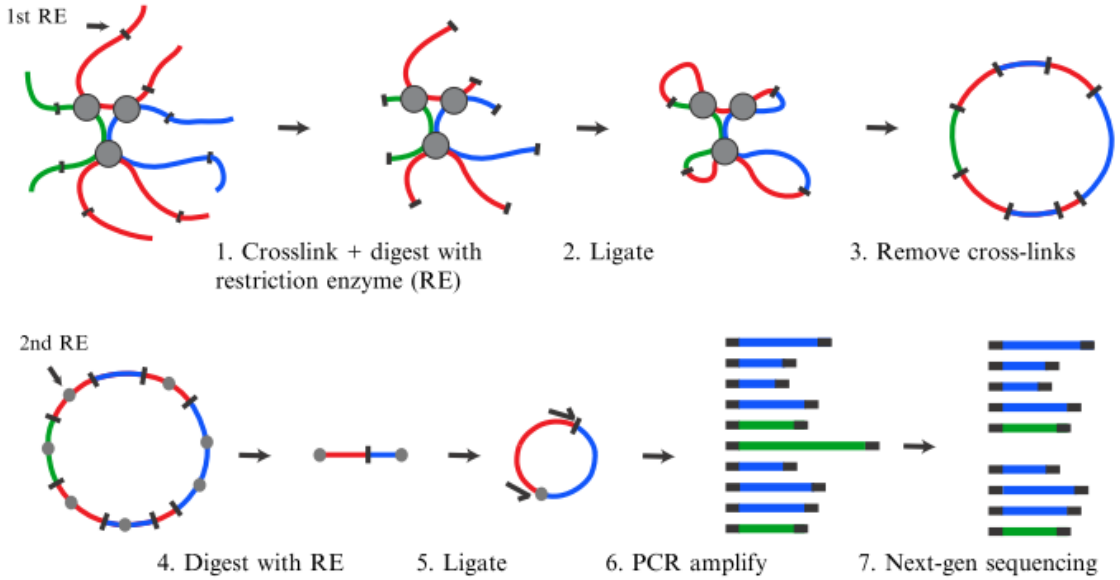

Figure 2.8: It shows general steps of 4C-Sequencing Technology**.** Two round restriction and ligation are applied, circular DNA samples are obtained for amplification and lastly PCR samples are sequenced and analyzed (Van De Werken et al., 2012).

GWA Studies have successfully identified variants and risk locus related to diseases, but their exact function and mechanism of action has not been fully elucidated. The fact that risk alleles are found mostly in non-coding genome regions makes it difficult to reveal their functional effects (Grob & Cavalli, 2018).

2.3 Disease Modelling with Induced Pluripotent Stem Cells (iPSCs) and Genome Editing

Understanding of disease physiopathology is still critical to improving novel therapies. Although related cell lines and animal models provide an important advantage, they have limitations on creating complex disease models. In the world, there are 10000 different monogenic diseases and number of complex diseases. Complex diseases have different genetic variants and they are also affected by environmental factors. Animal modelling is not sufficient, especially for complex diseases, to understand the basis of the underlying molecular mechanism of disease. Therefore, IPSCs (Induced Pluripotent Stem Cells) have been become new approach for disease modelling (Grandy, Tomaz, & Vallier, 2019). In last years, IPSC reprogramming and culture conditions have been optimized and usage of IPSC technology has become common. This provides a new perspective for biomedical research (Hockemeyer & Jaenisch, 2016).

In 2012, Jennifer Doudna and Emmanuelle Charpentier designed Cas9 protein that combined with sgRNA (single guide RNA) to alter the targeted genomic locus. After that, this genome editing technique was then applied and optimized to HPSC and IPS cell lines. Cellular versatility of IPSCs and their association with CRISPR/Cas9 mediated genome editing has become a very powerful experimental approach in stem cell research and models of human disease. The most exciting of experiments conducted by combining these technologies to date is to test the attack of empirical data generated by GWAS genetically and functionally. Because it is known that, when low frequency risk alleles associate with different mutations, the impact of disease may increase and it is important to develop new therapeutic approaches to understand mechanism of these risk alleles. Overall, combination of the power of IPSCs and genome editing has provided a point of view for analyzing main biologic process, cell immortality and neuronal biology.

3 MATERIALS AND METHODS

3.1 MATERIALS

3.1.1 Cell Lines

Used cell lines in this research to construct 4C-seq libraries and CRISPR/Cas9 was shown in **Table 3.1.**

Table 3.1: List of used cell lines to prepare 4C-libraries and CRISPR/Cas9

Cell Lines	Properties	Supplied From
U87	Human Primary Glioblastoma Cell Line	ATCC
HEK-293T	Human Embryonic Kidney Cell	ATCC
IHA- empty **IHA- wt** **IHA-R132H**	Immortalized Human Astrocytes + empty Tet ON vector +Tet ON with IDH-wt +Tet ON with IDH-R132H	Gift from Prof. Timothy A. Chan and Sevin Turcan (Turcan et al., 2018)
IPSCs	Induced Pluripotent Stem Cells	Applied Stem Cell #ASE-9202

3.1.1.1 Immortalized Human Astrocytes

Immortalized human astrocytes were gift from Prof. Timothy Chan by helping of Dr. Sevin Turcan. First of all, Sonoda and colleagues (Sonoda et al., 2001), used hTERT to immortalize normal human astrocytes. After that, Prof. Chan and colleagues modified these cells as doxycycline inducible IDH1-R132H and IDH1- wt (Turcan et al., 2018). At the end, 3 different cell lines were which are IHA-empty (containing mock plasmid), IHA cells with doxycycline inducible IDH1-R132H expression and lastly IHA cells with doxycycline inducible IDH1-wt expression. In this study, all these three cell lines were used for 4C-seq experiments and after 2-HG treatment, cells containing IHA-R132H were used for RNA sequencing.

3.1.2 Cell Culture Medium, Supplements and Materials

Cell culture main consumables such as tissue culture flasks, serological pipettes were supplied from Sarstedt (Germany). To culture cell lines Growth Medium, PBS (Phosphate Buffered Saline), FBS (Fetal Bovine Serum), P/S (Penicillin/Streptomycin), and AGS (Astrocyte Growth Supplement) were used. Additionally, Dox (Doxycycline) was used to be induced Tet ON vectors in IHA cell lines. These materials were listed in **Table 3.2.**

Table 3.2: List of used materials for cell culture

Materials	**Catolog Numbers**	**Supplier**
Low- Glucose DMEM	# 31885-023	Gibco
High- Glucose DMEM	#41965-039	Gibco
Astrocyte Medium	#1801	ScienCell
Heat Inactivated FBS	# 10500-064	Gibco
Penicillin Streptomycin	#151401-122	Gibco
Doxycycline hyclate	#D9891-5G	Sigma
Tyripsin-EDTA (0.25%)	#25200056	Gibco
mTeSR Basal Medium	#85851	STEMCELL Technologies
mTeSr 5X Supplement	#85852	STEMCELL Technologies
Knock-Out Serum	#10828-028	Gibco
DMEM-F12 (Glutamax in)	#31331028	Gibco
Dispase in DMEMF12	#07923	STEMCELL Technologies
Matrigel (high qualified)	#354277	Corning
Glutamax 100X	#35050	Gibco
MEM-NEAA	#11140-035	Gibco
Human FGF-basic	#100-18B-50UG	PeproTech
Y-27632 (ROCK Inhibitor)	#Y0503	Sigma
Human EGF	#100-15	PeproTech
PDGFAA	#PHG0035	Gibco
Laminin (Natural, Mouse)	#23017-015	invitrogen
SB431542	#72234	STEMCELL Technologies
N-2 (100X)	#17502048	Thermo Fisher
B-27 (50X)	#17504044	Thermo Fisher
Neurobasal Medium	#21103049	Gibco
rh Noggin	#78060	STEMCELL Technologies

3.1.3 Commercial Kits, Chemicals and Enzymes

Kits and chemicals used to prepare the 4C-seq library were shown in the **Table 3.3 and Cntn'd Table 3.4.**

Table 3.3 : List of used kits, chemicals and enzymes

Materials	**Catolog Numbers**	**Supplier**
Tris	#TRS003.500	BioShop
NaCl	#TK.170540.01000	Tekkim
EDTA	#EDT001.500	BioShop
NP-40	#E109-100ML	amresco
Triton X-100	#BP151-500	Fisher
Protease Inhibitor Coctail (100X)	# 5871	Cell Signaling
Glycine	#GLN002.500	BioShop
Agarose	#AGA003.500	BioShop
SDS	#SDS001.100	BioShop
Trizma-HCl	# T5941	Sigma
Nuclease Free Water	# BE51200	Lonza
NaAC (Sodium Acetate)	# 1.06268.0250	Merck
Glycogen	# R0561	Thermo Scientific
Ethanol	# 920.026.2500	Isolab
Gel Loading Dye, Purple (6X)	# 7025	New England Biolabs
Phenol	# 2821 E357-500ml	Amresco
Chloroform	# 102431-2500	Merck
Formaldehyde	#1.04003.2500	Merck
DTT (Dithiothreitol)	#D9779-DTT(5G)	Sigma
ATP (Adenosine 5'triphosphate)	#A7699-1G	Sigma
Magnesium Chloride	#TK.120290.01003	Tekkim
Restriction Enzyme Buffer 10X	# B7204S	New England Biolabs

Table 3.4: Cont'd List of used kits, chemicals and enzymes.

Materials	Catolog Numbers	Supplier
SafeView Classic	#G108	abm
Q5 High Fidelity Polymerase	# M0491L	New England Biolabs
1 kb DNA Ladder	# N3232S	New England Biolabs
100 bp DNA Ladder	#N3231	New England Biolabs
BfaI Restriction Enzyme	# R0568L	New England Biolabs
HindIII HF Restriction Enzyme	# R3104L	New England Biolabs
T4 DNA Ligase	# M0202L	New England Biolabs
Protinase K	# P81075	New England Biolabs
RNAse A	#R6513	Sigma
Deoxynucleotide (dNTP) mix	# N0447S	New England Biolabs
QIAquick PCR Purification Kit	# 28106	Qiagen
50X TAE Buffer	#TAE222.1	Bioshop

3.1.4 Used Oligos for this study

To amplify 4C Templates, used oligos and c-MYC and GAPDH qPCR primers for edited IPSCs were shown in **Table 3.5** and used gRNA to edit IPSCs' genome was shown in **Table 3.6.** Indicated gRNA was designed around SNP rs55705857 located at 8q24.21.

Table 3.5: Used Oligos for 4C PCR Reaction

Name of Oligos	Sequence from 5' to 3'
4C-reading primer (BfaI)	GGATTATACAGCATCACATGCCTAGAA
4C- nonreading primer (HindIII)	ATACTTCGAACTCCAGCCCTGCC
c-MYC Forward	CGCCGCCAAGCTCGTCTCA
c-MYC Reverse	AGGGGTCGATGCACTCTGAGGC
GAPDH Forward	TGCACCACCAACTGCTTAGC
GAPDH Reverse	GGCATGGACTGTGGTCATGAG

Table 3.6: gRNA sequence for genome editing. Bold underlined sequences shows Protospacer Adjacent Motif (PAM) sequences.

gRNA	Sequence from 5' to 3'
YH.106.CCDC26.g2	AACAAGTTCTTTACGTAAACGTC

3.1.5 Devices

During Cell Culture and 4C-seq library preparation some machines were used as listed in **Table 3.7**.

Table 3.7 : List of used devices

Devices	Supplier
Cell Culture Cabinet	Thermo Scientific
Heracell CO_2 Incubator	Thermo Scientific
Centrifuge 5810R	Eppendorf
SimliAmp Thermal Cycler	Applied Biosystems
pH meter	Hanna
GelDoc XR with Image Lab Software	Biorad
Electrophoresis System& Basic Power Supply	Biorad
Centrifuge MicroCL 17R	Thermo Scientific
Nanodrop 2000	Thermo Scientific
Axio Vert. All Inverted Microscope	ZEISS
Microvawe	Beko

3.2 METHODS

3.2.1 4C-seq Library Preparation

3.2.1.1 Cell Culture for 4C Library

As shown in **Table 3.1,** 5 different cell lines were used to prepare 4C –libraries for this project. Their own culture medium was prepared and used for each cell line. Cells were plated into T75 flasks; all was cultured at 37 ^{o}C and 5 % CO_2 in incubator.

For U87 cell line Low-Glucose DMEM containing 10% FBS and 1% P/S medium was prepared and for HEK-293T cell line same medium was prepared with high-glucose containing

medium. To culture astrocyte cell lines Astrocyte Medium was prepared as shown in **Table 3.8.** Doxycycline containing medium was used to induce Tet ON vector, all three astrocyte cell lines were cultured with separately with doxycycline containing astrocyte medium and normal astrocyte medium. This mutant, which can induce IDH1-R123H with dox confirmed by Western blotting using protein- specific antibodies.

Table 3.8: Preparing IHA Cells Medium

Normal Astrocyte Medium	**Doxycycline Containing Astrocyte Medium**
Astrocyte Media + 5 ml Astrocyte Growth Supplement (AGS) + 10 ml FBS + 5 ml P/S	Doxycycline was added freshly into Normal Astrocyte Media , last concentration as 1 ug/ml Doxycycline Preparation : 10 mg Doxycycline dissolved in 10 ml nuclease free water and it is prepared as stock concentration :1mg/ml

During 4C library preparation 4C Technology: Protocols and Data Analysis (Van De Werken et al., 2012) was followed, just for sequencing part of experiments, primers used without adapter sequences.

3.2.1.2 Cross-linking of Chromatin and Cell Lysis

In this part, lysis buffer was prepared freshly and kept in ice as shown in **Table 3.9** before starting cell fixation. For each cell line, $10x10^6$ cells were needed to prepare 4C library. 5 different cell lines and in total 8 different conditions that we had which are U87, 293T, IHA-empty Dox-, IHA- empty Dox +, IHA-wt Dox-, IHA-wt Dox+, IHA-R132H Dox- and IHA-R132H Dox+.

Cell counting was done and they were centrifuged at proper rpm for each cell line (U87; 1500 rpm for 3min, HEK-293T; 1400 rpm for 2min and IHA; 1200 rpm for 5 min.) Supernatant was thrown out and each pellet was resuspended in 5ml PBS/10% FBS mixture. After that, 5 ml 4% formaldehyde was added to the same falcon (the last concentration of formaldehyde was 2%), that cell pellet was resuspended, and incubated 10 minutes at room temperature while inverting for a few times. After 10 minutes incubation, 1425 ul of 1M Glycine was added to falcons and they were put in ice immediately to block cross-linking. Then, samples were

centrifuged at 1300 rpm for 4 min at 4º C. All supernatant was thrown out by using vacuum and pellet re-suspended in 5 ml prepared cold lysis buffer (Van De Werken et al., 2012).

Table 3.9: 10 ml Lysis Buffer Preparation

Contents for 10 ml Lysis Buffer	**Last concentrations**
500 ul of 1M Tris	50 µM
300 ul of 5M NaCl	150 µM
100 ul of 0.5 M EDTA	5 µM
250 ul of 20% NP-40	0.5 % NP-40
100 ul Triton X	1% Tx-100
100 ul of 100X Protease Inhibitors Cocktail	1X
8650 ul nuclease free water	
All is mixed as calculated amounts, and buffer was kept in ice.	

Then samples were incubated in ice for 10 minutes, after they were centrifuged at 1800 rpm for 5 minutes at 4º C. After centrifugation, supernatant was poured and at this stage, samples can be stored in -80 º C in 1,5 ml micro centrifuge tubes, first shock freezing of pellet in liquid nitrogen. On the other hand, experiment can be continued with digestion part.

3.2.1.3 Digestion of Cross-Linked Chromatin by Restriction Enzyme

After chromatin fixation and cell lysis were completed, 440-ul nuclease free water and 60 ul of 10X Restriction enzyme buffer were added to samples and tubes were incubated at 37ºC and then 15 ul of 10 % SDS was added to samples and samples were incubated at 37º C while shaking at 900 rpm for one hour. After that, 5 ul aliquot of these incubated samples were taken and they were kept as “undigested control”. At that point, digestion process was completed in three steps, these were; firstly added 200U, 10ul, HindIII HF restriction enzyme and shaken at 900 rpm for 4 hours at 37º C, secondly enzyme was added again and at same conditions samples incubated for overnight and lastly enzyme was added and incubated for four hours under the same conditions. After digestion was completed 5ul aliquots were taken from samples as “digestion control”.

3.2.1.4 Digestion Efficiency Control

Then "undigested control" samples and "digestion control" samples were prepared to analyze digestion efficiency before continuing to rest part of protocol. For this 90 ul of Tris-HCl, concentration was 10 mM and pH 7.5, was added to 5 ul of control samples and then 2,5 ul of Proteinase K was added, concentration was 20 mg/ml, and samples were incubated at 65^{o} C for 1 hour. After incubation was completed, 20 ul of prepared samples were loaded on 0.6% agarose gel, preparation as shown in **Table 3.10,** if digestion efficiency was not sufficient to continue to processing, all digestion part should be repeated.

Table 3.10 : Agarose Gel Preparation for Gel Electrophoresis

Contents	**Preparation**
0.6% Agarose Gel 0.6 gram agarose 100 ml 1X TAE (Tris-Acetate-EDTA) Buffer 10 ul SafeView **1.5% Agarose Gel** 1,5 gram agarose 100 ml 1X TAE (Tris-Acetate-EDTA) Buffer 10 ul SafeView	First, Proper amount of agarose was weighted and then put in 100 ml 1X TAE Buffer, after that, solution was heated in microwave until no agarose particle was seen. It was allowed to cool slightly then 10% percent SafeView was added and poured in Electrophoresis Gel Tank , after gel becoming solid, 1X TAE Buffer was filled into tank. Power Supply was connected and samples were run at 75 V for about 1 hour. Lastly, gel was removed from running box carefully and samples were visualized under UV light.

3.2.1.5 Ligation Protocol for Cross Linked DNA fragments

After the digestion efficiency was observed as expected, the activation of the restriction enzyme was inactivated at 65^{o} C by 20 minutes of incubation. After that, samples were transferred into 50 ml falcon tubes, 700 ul of 10 X ligation buffer, as shown **in Table 3.11**, was added, and then samples volumes were completed to 7 ml by adding nuclease free water. Then, 9 ul of T4 DNA ligase was added, last concentration was 5U/ul, and incubated at 16^{o} C for overnight.

Table 3.11 : Preparation of 10X T4 DNA Ligase Reaction Buffer

Contents and Last Concentration	Preparation
50 mM Tris-HCl 10 mM $MgCl_2$ 1mM ATP 10 mM DTT (Dithiothreitol)	To prepare 6 ml 10 X Ligation Buffer; 0,036 gram ATP 0,12 gram $MgCl_2$ were weighted, 600 ul 1M DTT and 3 ml of 1M Tris-HCl were added and solution volume was completed to 6 ml by adding nuclease free water.

3.2.1.6 Ligation Efficiency Control

After the ligation was completed, 100 ul aliquots of "ligation control" were taken and 2,5 ul of Proteinase K (20 mg/ml) was added to these aliquots, then they were incubated at 65^o C for one hour. At the following part, samples were loaded to 0.6% agarose gel, as shown in **Table 3.9.** If ligation efficiency was sufficient, the rest of the protocol can be applied, however, fresh ATP should be added and the ligation protocol should be repeated.

3.2.1.7 Reversing of Cross-Links

To reverse cross-link of DNA fragments 15 ul ProtK (10mg/ml) was added and incubated at 65^o C for overnight, then 3 ul RNAse A, concentration was 100mg/ml, was added and incubation was proceed during 45 minutes at 37 ^{o} C. After that part, 1:1 ratio phenol: chloroform was prepared and 7 ml was added to each sample. They were centrifuged at 3300 g for 15 minutes at room temperature. After centrifugation, water phase was transferred to new 50 ml falcon tube and 7 ml nuclease free water, 1, 5 ml of NaAC (2M, pH 5, 6) and 35 ml 100% ethanol were added and after mixing samples were kept at -80^o C until the samples were fully frozen. Frozen samples were centrifuged at 8300g for 20 minutes at 4^o C. Thereafter, supernatant was poured and 10 ml of cold 70% ethanol was added onto pellets, they were centrifuged again at 3300 g for 15 minutes at 4^o C. Supernatant was removed and pellets were dissolved in 150 ul of Tris-HCl (10 mM concentration, pH 7,5). At this point, samples can be stored at -20 ^{o} C. These samples are named as "3C" sample.

3.2.1.8 Adjustment the size of constructed DNA circles (Secondary Digestion and Ligation)

3C samples were taken and for second digestion, 50 ul 10X restriction enzyme buffer was added to samples and 5 ul (50U) of BfaI restriction enzyme was added, then volume of reaction volume was completed to 500 ul and incubated at 37^{o} C for overnight. After incubation, 5 ul restricted samples were taken as "digestion control" samples and digestion efficiency was checked as explained in the "Digestion Efficiency Control" section. When digestion was adequate, the restriction enzyme was inactivated and samples were transferred to 50 ml of falcon tubes. Later on, as shown in **Table 3.10**, 1,4 ml of Ligation Buffer (10x), 18 ul T4 ligase (100U) were added and sample volumes were completed using 14 ml nuclease free water. For ligation, samples were incubated at 16^{o} C for overnight. Subsequently, 1,4 ml of NaAC (2M, pH 5.6), 14 ul of glycogen and 35 ml 100% ethanol were added and samples were kept at -80^{o} C, until they were wholly frozen. Frozen samples were centrifuged at 8300 g for 20 minutes at 4^{o} C. Supernatant was thrown away and then 15 ml of cold 70% ethanol was added to pellets. Centrifugation was done at 3300g at 20^{o} C for 15 minutes. Post- centrifuge , supernatant was poured and pellet was dried at room temperature completely. Lastly, pellets were dissolved in 150 ul of Tris (10 mM, pH 7,5).

3.2.1.9 Sample Purifying by QIAquick PCR purification Kit

Each sample was divided into as 50 ul in 3 aliquots. 5 volumes of (250 ul) Buffer PB was added to samples and mixed (mixture color should be yellow, showing correct pH). Then samples were loaded into the spin column of QIAquick and centrifuged for 30-60 seconds at 13000 rpm. Flow-through was discarded and 750 ul Buffer PE was added for washing samples, and centrifugation was completed under the same conditions. Flow-through was poured again and at same conditions, empty centrifuge was done for another minute to remove alcohol contamination. Finally, DNA was eluted by adding 50 ul of Buffer EB (10 mM Tris-HCl, pH 8, 5) to the columns and centrifugation for one minute. Nanodrop measurement was subsequently completed and samples were kept at -20°C.

3.2.1.10 Primer Designing for 4C-Templates

To amplify 4C interacting region, primers were designed according to inverse PCR conditions, these primers can be called as "reading primer" and "non-reading primer". Primers were designed with enzyme cutting points in mind. The second restriction enzyme was BfaI and one primer should be located between 20 bp away from this restriction site, and the second

primer should be located nearly 100 bp away from the HindIII restriction site. Designed oligos have been shown in **Table 3.5.** They should be located in the region of viewpoint.

3.2.1.11 PCR (Polymerase Chain Reaction) amplification of 4C Templates

Before reaction set-up 12,5, 25,50,100 and 200 ng PCR templates were tried to optimize the amplification process. After optimizing all PCR protocols for 8 samples, 10 PCR reactions were set up in 25 ul volumes as shown in **Table 3.12**. Reactions were set up as shown in **Table 3.13**. All experiments were repeated three times.

Table 3.12: PCR Reaction Components with Q5 High Fidelity Polymerase

Components	**Amount**
5X Reaction Buffer	5 ul
5X GC Enhancer	5 ul
10 µM Reading Primer	3,5 ul
10 µM Non-Reading Primer	3,5 ul
dNTP mix	0,5 ul
4C DNA Template	250 ng
Q5 High Fidelity DNA Polymerase	0,5 ul
Nuclease Free Water	Up to 25 ul

Table 3.13: PCR Conditions

Cycle	**Temperature**	**During time**	**Number of Cycles**
Initial Denaturation	98 ° C	30 sec	1
Denaturation Annealing 1 &Annealing 2 Extension	98 ° C 57 ° C & 61 ° C 72 ° C	10 sec 45 sec & 45 sec 2 min	35
Final Extension	72 ° C	2 min	1

3.2.1.12 Mini Seq Sequencing of Prepared 4C Samples and IGV_2.5.0 Analyzing

Prepared 10 reactions of 4C-PCR reactions, for each samples, were collected in one tube and samples were purified as described in section "3.2.1.9 Sample Purifying by QIAquick PCR purification Kit". All samples are diluted in 50 ul 10 mM Tris-HCl (pH 7, 5). Then, samples were sequenced using Illumina MiniSeq System. For this part, MULTIGEN Health

Service helped us for sample sequencing. First, they prepared the cartridge for the reagent. The prepared library was then denatured and diluted. Because the loading volume of the MiniSeq system loading volume should be 500 ul and the concentration should be 1.8 pM. MiniSeq System Guide was followed during loading and sequencing library (Illumina, 2018). After sequencing, they obtained BAM files and sent us. The obtained BAM files were scanned for all three replicates using IGV_2.5.0, the Integrative Genomics Viewer, the risk region and the expected interaction regions were scanned and Human hg19 database was used as the reference genome.

3.2.2 CRISPR/Cas9 Editing of IPS Cell Line

3.2.2.1 Designing gRNA and Validation

"Applied Stem Cell" company in US performed CRISPR/Cas9 genome editing on IPS cells. Firstly, several guide RNAs (gRNA) were designed nearly SNP rs55705857 at 8q24.21 as shown in **Figure 3.1.** For cell lines project, normalized NHEJ frequency is determined as equal as or bigger than 15 %, so YH106.CCDC26.g2 was used for transfection process, sequences were shown in **Table 3.6**. For this guide RNA, normalized NHEJ was found as 26,6% as shown in **Figure3.1.**

Figure 3.1: Designing and validation of gRNA to edit rs55705857- A alleles at 8q24.21 region. As shown in graph, gRNA activity via NGS, normalized by NHEJ frequency resulted from gRNA free transfection. And g02 reached to 26.6 % normalized NHEJ value.

3.2.2.2 Transfection and Selection of IPS Cells

IPS cells were transfected by using Neon Transfection system of Life Technologies. After transfection, IPSCs were cultured in matrigel coated 6-well tissue culture plates. Used

plasmid containing Cas9 also have resistance to puromycin. Transfected IPSCs were therefore exposed to selection of puromycin. Selection conditions were 0.1 ug/ml in 48 hours. After 48 hours, cultivated IPSCs were transferred to 48-well tissue culture plates and daily media changes were made until sufficient colonial was reached. Isolated IPSC colonies were genotyped for the insertion of homozygous point mutation at SNP rs55705857 and homozygous (G/G) allele confirmed by clone sequencing.

3.2.2.3 Maintenance of IPSC G/G and A/A Colonies

Applied Stem Cell Company converted rs55705857 A/A allele to G/G allele successfully. Firstly, MEF cells were grown on 0.1% gelatin coated plates and they should be plated in equal numbers. After reaching a confluence of 85%, mitomycin-C (last concentration: 10 ug/ml) containing MEF Media was replaced with normal MEF-conditioned media and cells were incubated at 37°C with 5% CO_2 for three hours in the incubator. After that, IPSCs were opened on this mitomycin positive MEF coated 6-well plates. IPS cells are grown in HeSC media as shown in **Table 3.14**. Cells were incubated until colonies reached sufficient size. Dispase is used to passage IPSCs and after first growing cells can be maintained on matrigel coated plate by changing media as mTeSR as shown in **Table 3.14.** Cell should be stay as colonies, so centrifugation should be at 0,1 rcf for two minutes. When IPSCs were cultured on MEF cells, just for first day Y- Compound (last concentration was 10 μM) should be added into b-FGF containing HeSC media to enhance adhering of IPSC onto MEF coated 6-well plates.

3.2.2.4 Genome Edited IPSCs Differentiation to ONPCs (Oligodendrocyte Neural Progenitor Cells)

For differentiation protocol was followed , prepared by Shi and colleagues (Shi, Kirwan, & Livesey, 2012). In order to differentiate IPSCs A/A and IPSCs G/G alleles containing cells into ONPCs, continued IPS cells were grown twice on MEF cells and cells allowed to proliferate during 6-10 days. Then, cells in 5 wells of 6 well plate were removed by dispase and collected in matrigel coated one well 12 well tissue culture plate. They should be confluent, and they should reach 100% confluency after 1 day. On matrigel coated plate, MEF-Conditioned Media contained 10 ng ml^{-1} , as shown in **Table 3.14,** was used until they completely cover the surface.

Table 3.14: Used medium for maintenance differentiation of genome edited IPSCs.

Name of used Media for Cell Culture	**Preparing Media**
HeSC media (200ml) (Human Embryonic Stem Cell Media)	156 ml DMEM-F12 Media, 40 ml Knock-out Serum 3 ml HEPES (15mM las concentration) 364 ul β-mercaptoethanol (55μM stock) 2 ml MEM-NEAA (100X) All mixed and filtered with 0,2 mm filtered system Before using media, Bfgf was added freshly into medium, last concentration is 100 ng/ml
MEF Media (50ml)	43 ml High-Glucose DMEM 5ml FBS 0,5 ml P/S, 0,5 ml Glutamax, 0,5 ml Sodium Pyruvate (100X), 0,5 ml MEM- NEAA(Non-essential amino acids, 100x), All mixed and filtered with 0.2 mm system.
mTeSR Media 50 ml)	40 ml mTeSR Basal Media + 10 ml 5X mTeSR Supplement (filtered with 0.2 mm filter system)
MEF Conditioned Media	MEF cells were cultured in normal MEF Media after they reach 85 % confluency, medium was changed with HeSC media without b-FGF, every day medium was collected and filtered, then fresh medium was added onto same cells during 6 days. Before this MEF Conditioned Media added onto IPSC cells, b-FGF was added freshly(10 ng/ ml)
N-2 Medium	DMEMF12(Glutamax), 1X N-2, 5 μg/ml Insulin, 1mM L-Glutamine, 100 μM MEM-NEAA, 100 μM 2-β Me, 50 U ml^{-1} Penicillin , 50 U ml^{-1} Streptomycin
B-27 Medium	Neurobasal Medium, 1X B27, 200 mM L-Glutamine, 50 U ml^{-1} Penicillin , 50 U ml^{-1} Streptomycin
Neural Induction Media	1:1 , N-2: B27 media containing 500 ng ml^{-1} Noggin and 10 μM SB431542 or

After cells reached to 100% confluency, medium was changed with Neural Induction Media as shown in Table 3.14. Neural Induction was continued during 8-12 days, while medium changed in every 24 hours. When morphology of cells turned to smaller nuclei containing neuroepithelial cells, cells were removed by dispase and cells were cultured on laminin-coated tissue culture plates. After that point, Neural Maintenance Medium was used (1:1, N-2: B27 medium). Until neural rosettes were formed, neural maintenance medium was used and then 20 ng ml $^{-1}$ was added medium and culture was maintanenced for additional 2-4 days. After that point, cells were proliferated on laminin coated plates.

3.2.3 Analysis of transcriptome changes dependent on 2-HG by RNA-Seq

IHA- R132H cells were treated with 2-HG to mimic the effect of R132H mutation on astrocytes. For that, during 72 hours, IHA cells were treated with 5nM 2-HG. Cells were collected from different wells and the isolation of RNA was completed for each well. After that, quality of RNA was analyzed by Bioanalyzer 2100 and nanodrop. Then, two wells were selected for 2-HG treated and untreated and their RIN values were greater than eight. Samples were sent for sequencing in dry ice. Sequencing was done as a base of 1x50 and 30 million reads were done. As a result of sequencing, raw RNA sequence data were checked for quality by fastqc. Array data was good quality and clean, so alignment step could be accomplished without any manipulation. The sequences of RNA were aligned with HISAT2 with the reference genome of Human Grch37. Annotation was performed by stringtie with aligned arrays from HISAT2. The files were created as a result of the annotation were merged and the file format required for the next step was created. The process up to this was done with the Linux terminal screen shell commands. After this step, differential expression analysis of the samples was performed using ballgown library in R script language. Enrichr web-based analysis tool was used to understand which genes, pathways and processes associated with 2-HG-dependent expression differences.

3.2.4 Analysis of MYC expression in IPSC-AA/GG by qPCR

RNA Isolation of IPSC-AA/GG cells was performed and cDNA was synthesized using standard protocol “NEB 1st strand cDNA synthesis kit”. Then these cDNAs were diluted to the same concentrations. For each well, 10 ul SybrGreen mixture, 0,5 ul of each primer, 4 ul of nuclease free water and 5 ul of cDNA were mixed and three replicates were performed for each cell line. Standard Promega RT Protocol was used for preparation and anlysis was done by Roche Light Cycler 480 .

4 RESULTS

4.1 4C-Seq Library Preparation Restriction and Ligation Gel Result Examples

4C library preparation experiments were started with parts of digestion and ligation. As full smear was expected, according to 4C protocols in literature for image of sufficiently digested samples, and after ligation DNA pieces become together and the size of DNA pieces become greater and partially smear view shifted to the upper site of agarose gel as shown in **Figure 4.1.** Digestion and ligation steps are critical to the preparation of the 4C-seq library.

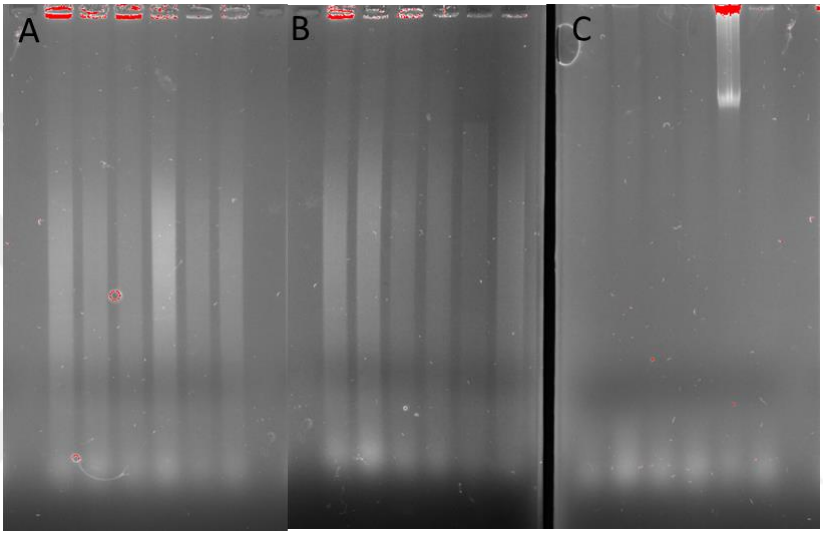

Figure 4.1: Figure shows restriction and ligation gel results examples. A) First restriction of astrocytes with HindIII restriction enzyme. B) Second restriction of astrocytes with BfaI restriction enzyme. C) First ligation gel results of astrocytes. Gel electrophoresis was done on 0.6 % agarose gel.

4.2 4C-Seq PCR Trials to Optimize Amplification Process

4C library preparation experiments were continued with PCR amplification process as mentioned in section **3.2.1.11.** To optimize the amplification process, concentrations of 12,5, 25, 50, 100 and 200 ng DNA were tested as shown in **Figure 4.2**. 200 ng DNA concentration showed the best PCR amplification template to prepare 4C library. Optimization was performed with HEK-293T cell line and other PCR reactions were performed under conditions were shown in **Table 3.12** and **3.13.**

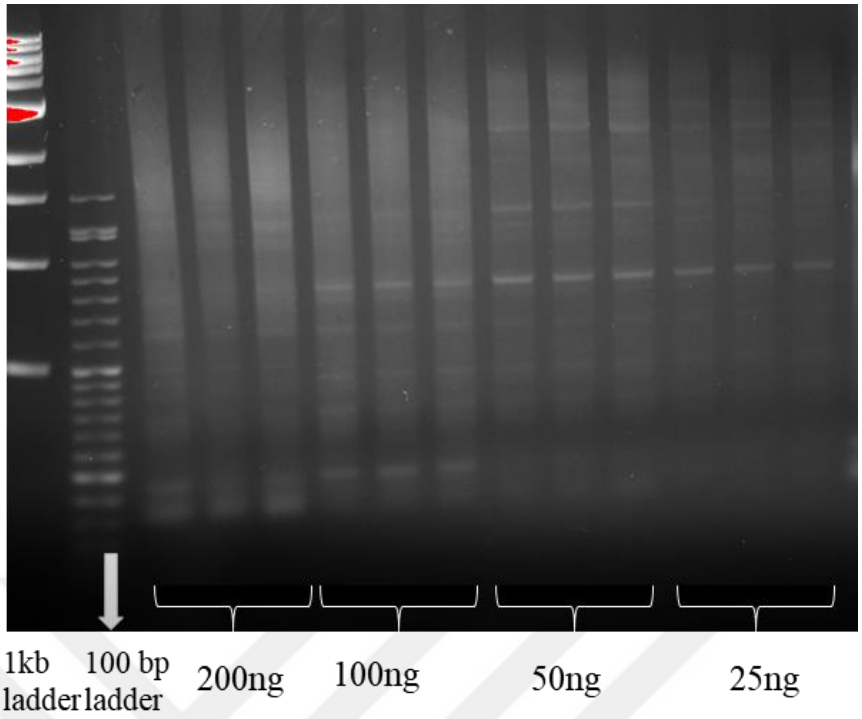

Figure 4.2: PCR Dilution Curve of 4C experiments is shown in figure. The HEK-293T cell line was used to optimize PCR reactions and 200 ng DNA shows the better amplification. When DNA concentration was low such as 25 ng, amplification worked in poor yield. It was possible to show reactions with 200 ng DNA as overloaded, but after the PCR purification step this almost entire smear view will disappear and expected bands can be better observed.

4.3 4C-Seq Last PCR Gel Results

Afterwards, Optimized PCR conditions were applied for all eight different cell lines. 10 reactions were prepared in 25 ul volume by using 200 ng DNA and then all reactions were collected separately for each cell line and purified with QIAquick PCR purification kit as mentioned in section **3.2.1.9.** After that, purified PCR samples were checked using 1,5 % agarose gel and 1 kb ladder was used as reference before sequencing. Letters on agarose gel image referred to used cell lines as A : IHA- R132H-Dox-, B : IHA - R132H- Dox +, C : IHA – wt – Dox +, D : IHA – wt – Dox -, E : A – empty – Dox - , F : IHA – empty – Dox +, G : U87 an lastly H : HEK-293T as shown in **Figure 4.3.**

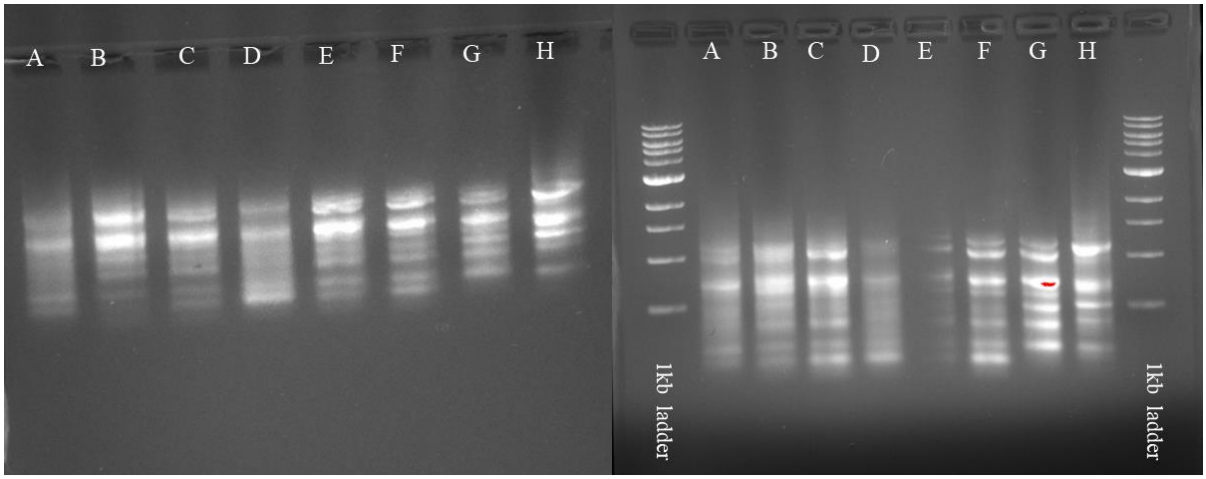

Figure 4.3: Figure shows two of 4C-Sequencing last purified PCR samples agarose gel examples before sequencing. A: IHA- R132H-Dox- , B: IHA - R132H- Dox +, C: IHA – wt – Dox+, D: IHA – wt – Dox - , E: IHA – empty – Dox - , F: IHA – empty – Dox +, G: U87, H: 293T.

4.4 Analysis of 4C-Sequenced Data by IGV.

After BAM files were obtained these datas were aligned by using IGV_2.5.0 integrative genomic viewer and area from 8q24.12 to 8q24.3 region as shown in **Figure 4.4**. Hg19 (GRCHh37.p13) human genome was used as reference genome. Some of the interacted regions found were shown in all three replicates, were labeled as interacted regions in NCBI Genome Data Viewer.

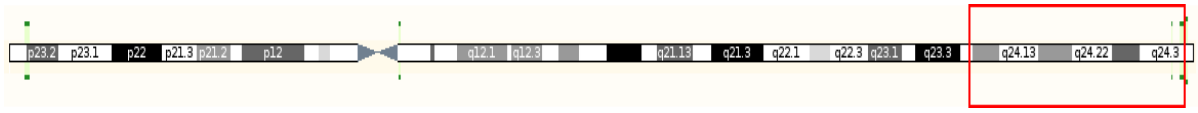

Figure 4.4 : Figure shows the scanned region on chromosome 8 by IGV.

BAM files of three replicates of each cell line were analyzed and interacted regions were identified. When these regions were chosen, mainly three criteria taken into consideration that were bam coverage values (read counts) were chosen as bigger than 40, read quality was at least 60 and alignments were shown in two of three replicates. These criteria were applied during analysis of all eight-cell lines. Firstly, BAM files of three replicates of IHA-R132H-dox - cells were analyzed as shown in **Figure4.5** and **Figure 4.6.**

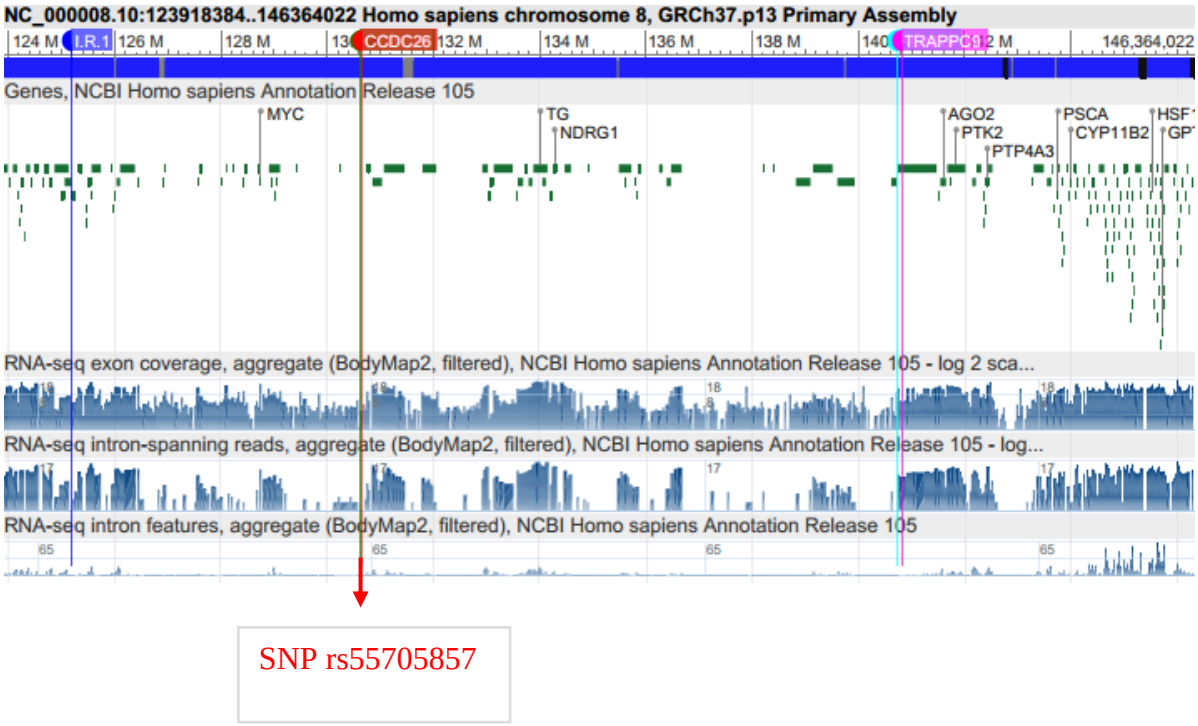

Figure 4.5: (IHA-R132H-Dox-**)** Range is between chr8:124000000-146365000**.** Five interacted regions were identified; one of which was labeled as IR1 (interacted region1), it is located at chr8:125184240-125184279 and it did not refer any gene. Two of which were in CCDC26 genomic region, one of which was in TRAPPC9 (transport protein particle complex 9) and last in KCNK9 (potassium two pore domain channel subfamily K member 9) on NCBI Genome Data Viewer.

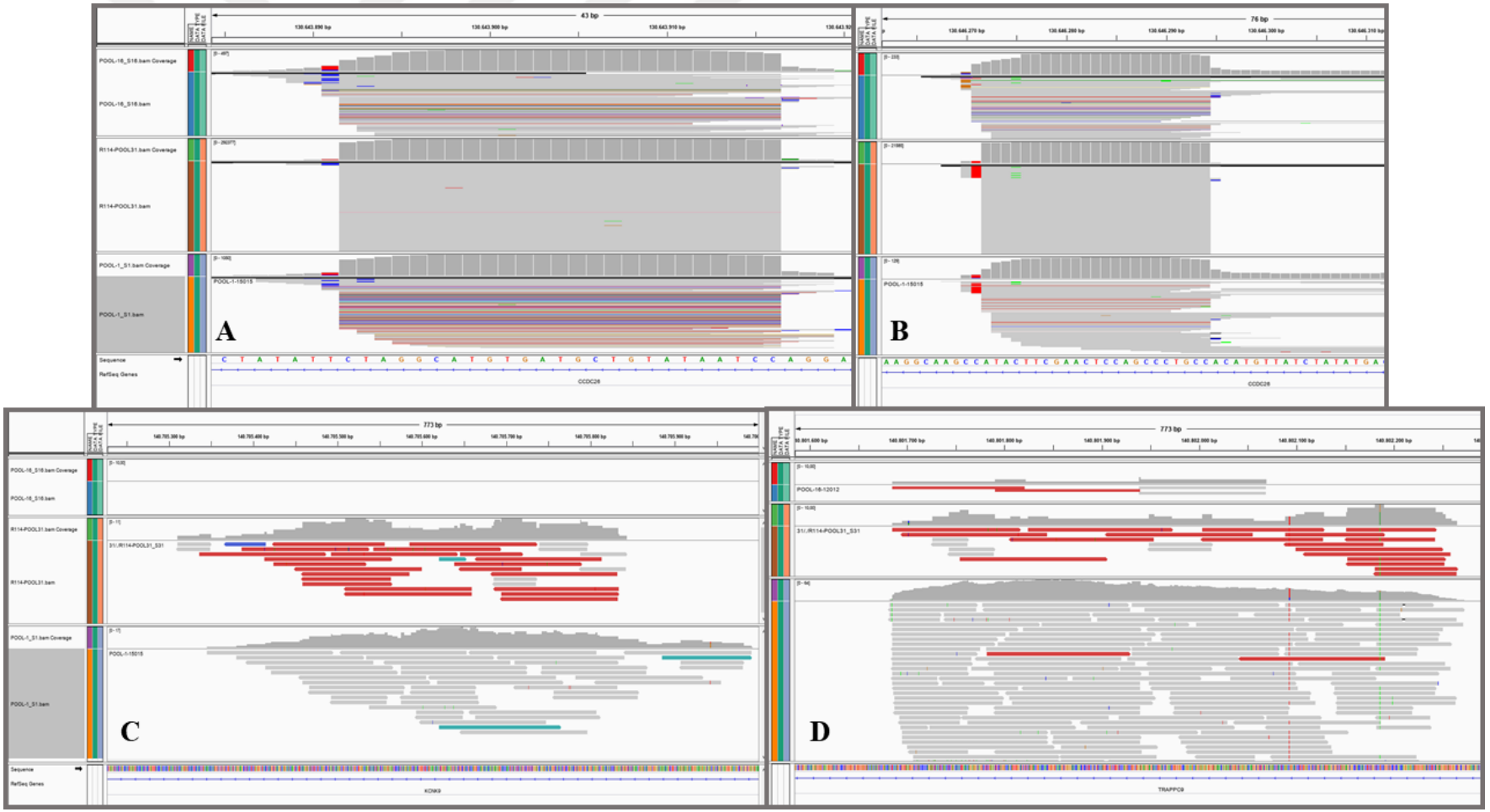

Figure 4.6: Figure shows IGV 2_5_0 images of IHA-R132H-Dox- interactions, four of five region were shown. A: chr8:130643883-130643922(CCDC26), B: chr8:130646262-130646337 (CCDC26), C: chr8:140705227-140706003(KCNK9), D: chr8:140801585-140802361 (TRAPPC9).

Secondly, IHA-R132H-Dox+ cells were analyzed and six interactions were identified. Locations of regions were labeled on NCBI Genome Data Viewer as shown in **Figure 4.7** and IGV2_5_0 images of some of interacted regions were shown in **Figure 4.8.** Interactions of KCNK9, TRAPPC9 were stronger than IDH-R132H-dox- cells Additionally TRIM28 interaction was found. Interactions where non-coding regions were different between dox- and dox+ IHA-R132H cells by using IGV2_5_0. Then we compared differences between Dox- and Dox+ cells of IHA-R132H as shown in **Figure 4.9.**

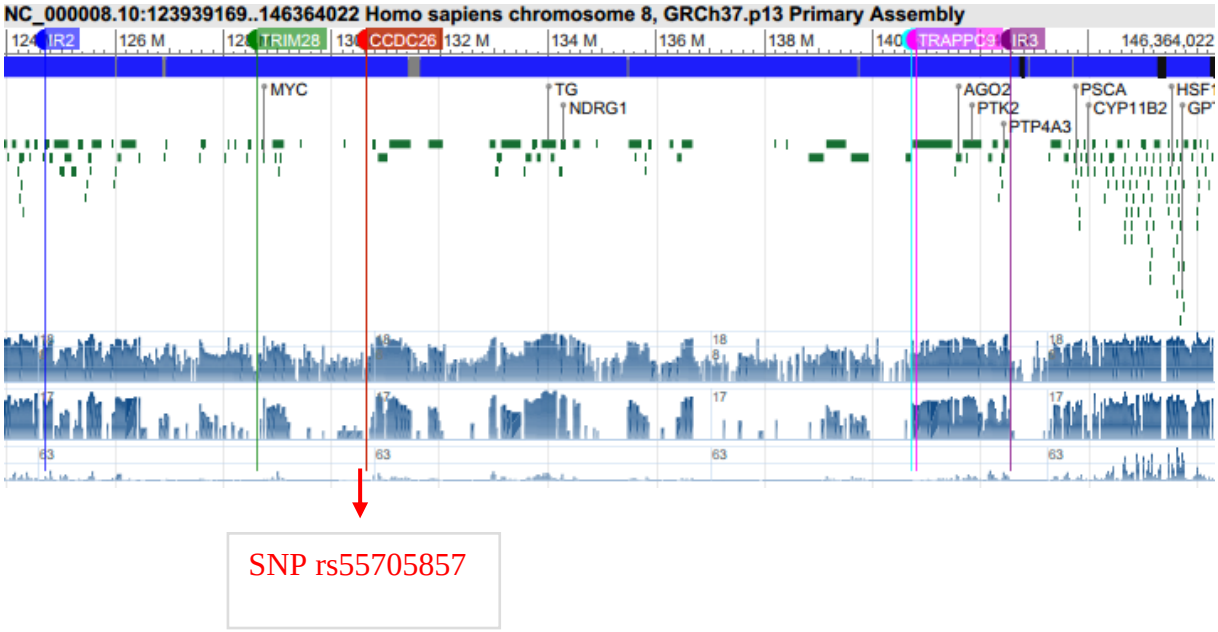

Figure 4.7: (IHA-R132H-Dox+**)** Range is between chr8:124000000-146365000. Six interacted regions were identified and shown; one of which was labeled as IR2 (interacted region2) it is located at chr8: 124696906-124707243, it did not refer any gene. Two of which were in CCDC26 genomic region, one of which was TRIM28, one of which was in TRAPPC9 (transport protein particle complex 9) and last in KCNK9 (potassium two pore domain channel subfamily K member 9) on NCBI Genome Data Viewer.

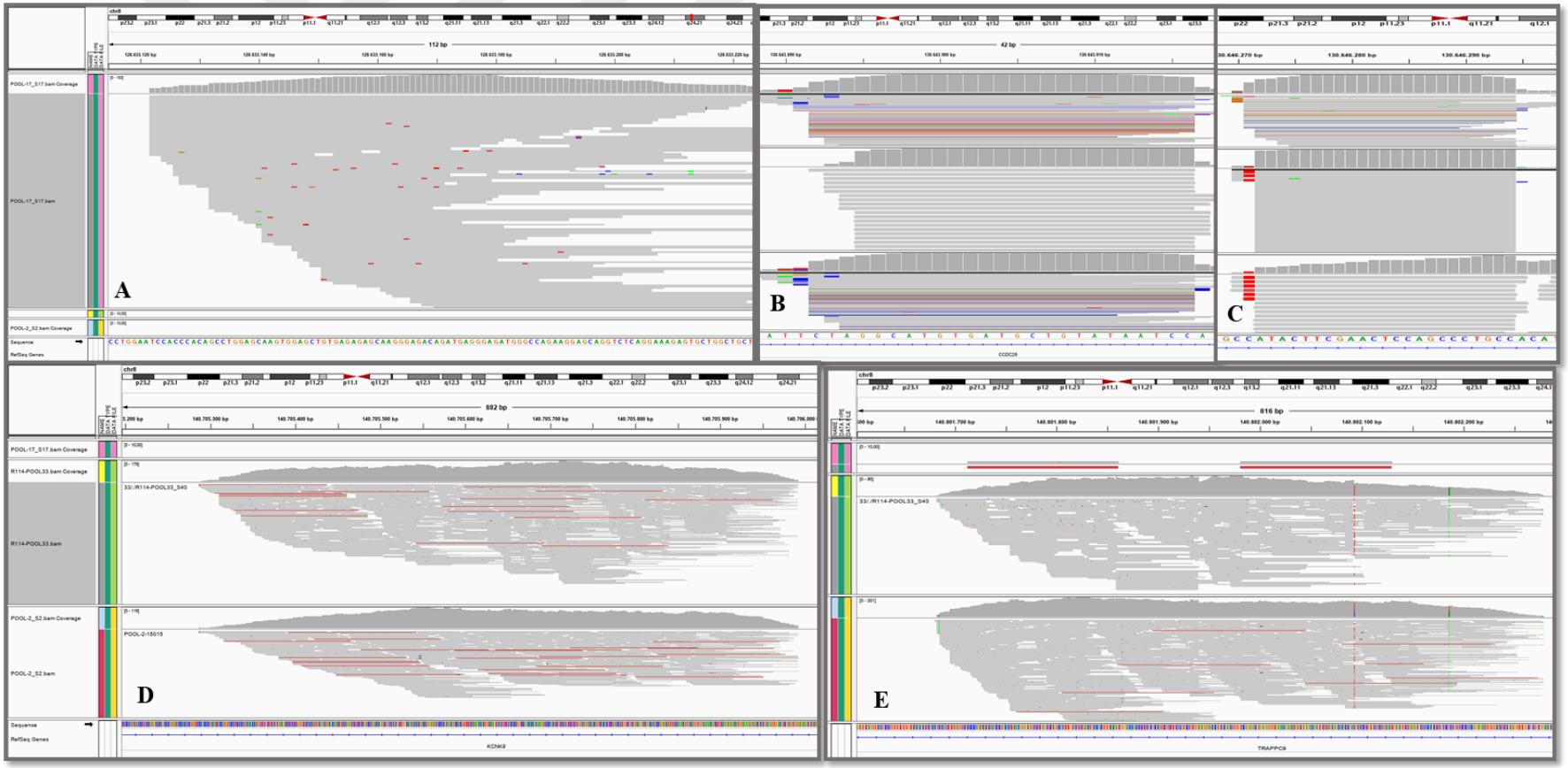

Figure 4.8: Figure shows IGV 2_5_0 images of IHA-R132H-Dox+ interactions, five of six region were shown. A: 128633047-128633307 (TRIM28) B: chr8:130643883-130643922(CCDC26), C: chr8:130646262-130646337 (CCDC26), D: chr8:140705227-140706003(KCNK9) and E: chr8:140801585-140802361 (TRAPPC9).

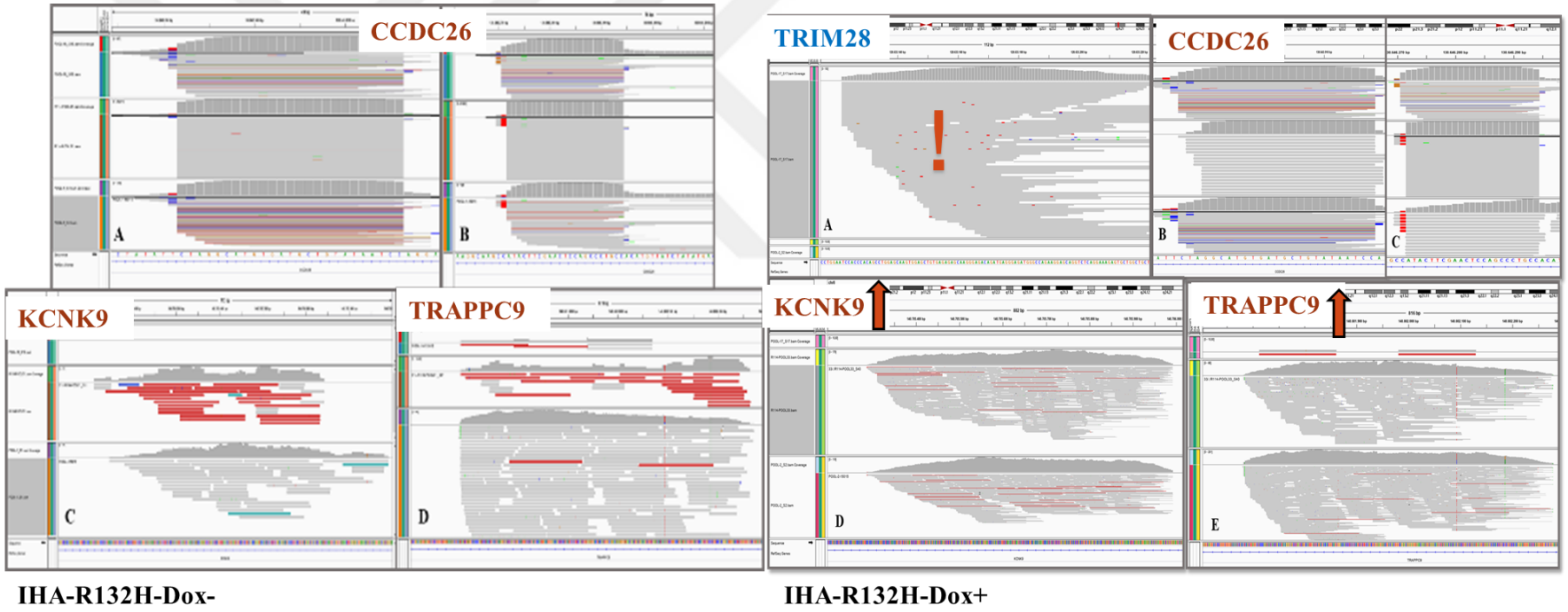

Figure 4.9: Figure shows the some differences and similarities between Dox- and Dox+ IHA-R132H cells. Differentially interacted MYC regulator region (TRIM28) was shown differentially in Dox+ cells and interactions of KCNK9 and TRAPPC9 were shown as increased in Dox+ IHA-R132H cells.

Thirdly, IHA-wt-Dox- cells were analyzed and five interactions were identified. Locations of regions were labeled on NCBI Genome Data Viewer as shown in **Figure 4.10** and IGV2_5_0 images of some of interacted regions were shown in **Figure 4.11.** As differently, significant interactions were not observed in non-coding region as IHA-R132 cells. TRIM 28 expression was lower than IHA-R132H-Dox cells as determined in IGV_2_5_0.

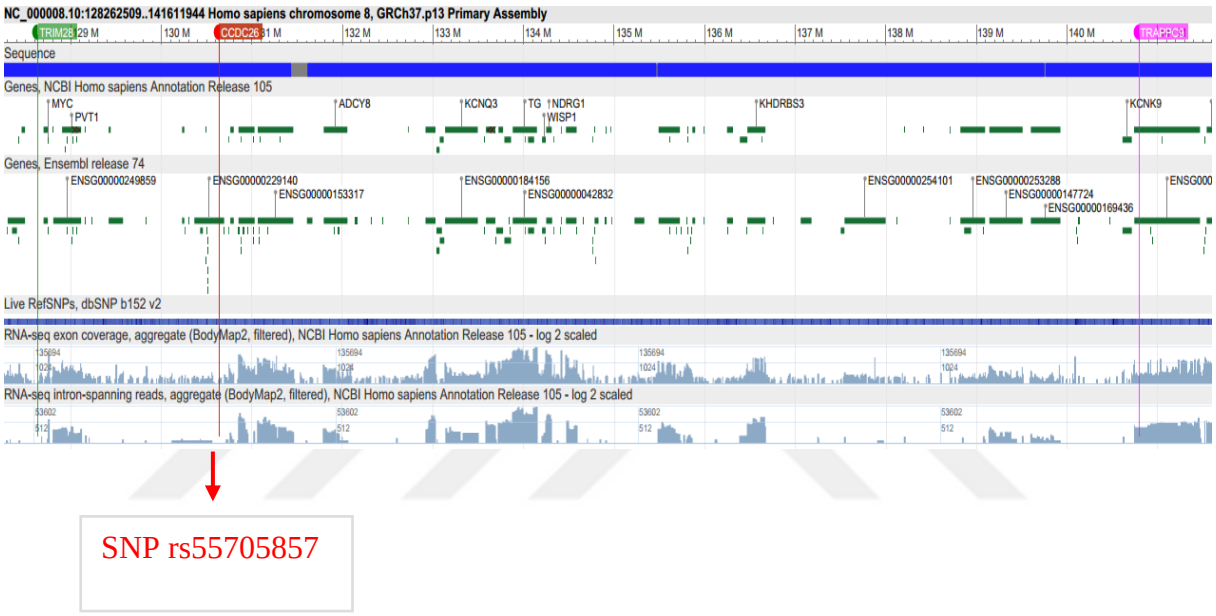

Figure 4.10: (IHA-wt-Dox-**)** Range is between chr8: 128262510:141611944. Five interacted regions were identified and illustrated. Two of which were in CCDC26 genomic region, one of them was TRIM28, last one was in TRAPPC9 (transport protein particle complex 9) on NCBI Genome Data Viewer.

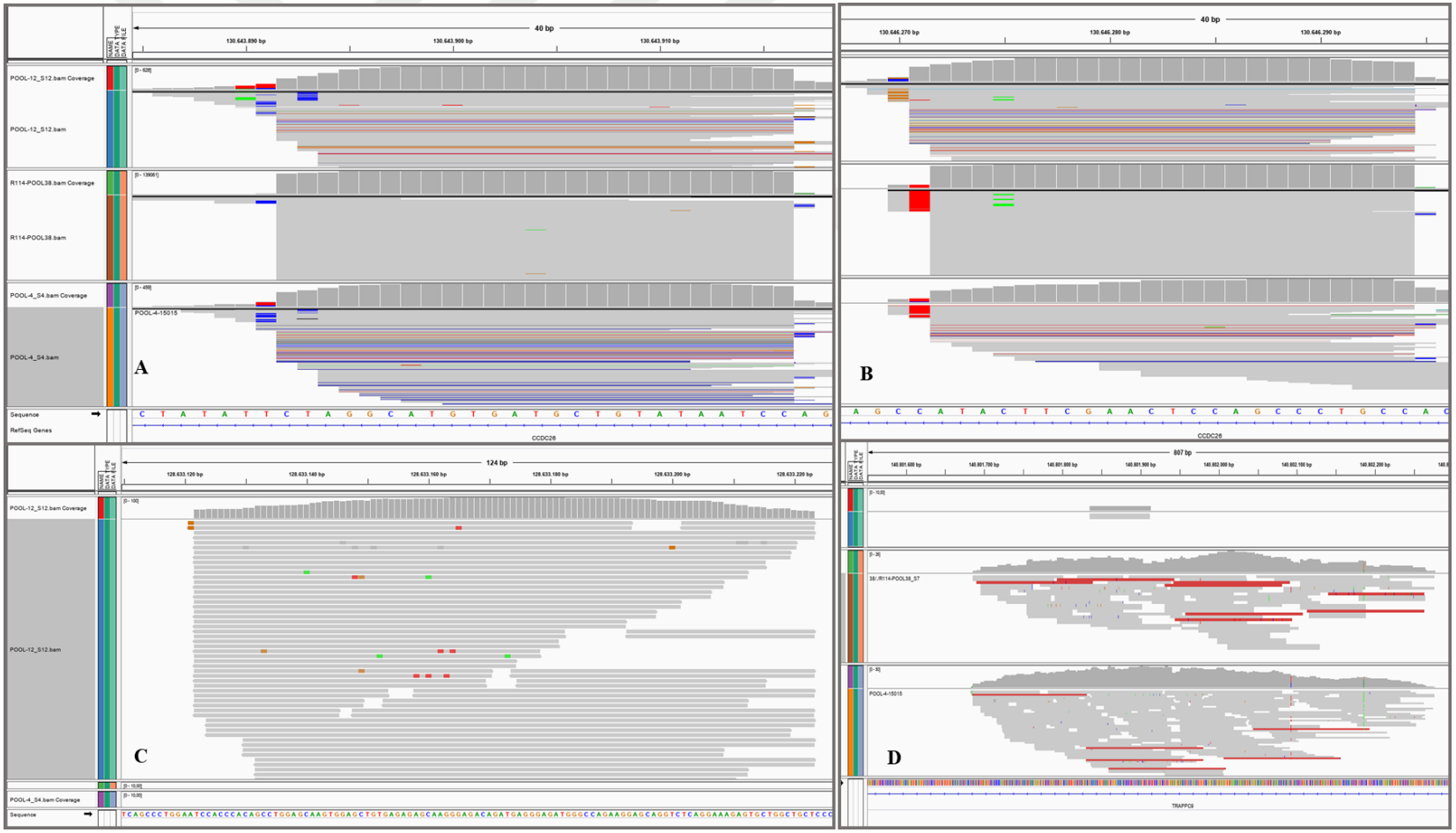

Figure 4.11: Figure shows IGV 2_5_0 images of IHA-wt- Dox- interactions. Four of five region were indicated. A: chr8:130643883-130643922(CCDC26), B: chr8:130646262-130646337 (CCDC26), C: 128633047-128633307 (TRIM28) and D: chr8:140801585-140802361 (TRAPPC9).

Fourthly, Analysis of IHA-wt-Dox+ cells were completed at determined risk region and six interactions were identified. Found regions were labeled on NCBI Genome Data Viewer as shown in **Figure 4.12** and IGV2_5_0 views of a couple of interacted regions were indicated in **Figure 4.13.** As differently, significant interactions were not observed in non-coding region as IHA-R132 cells. Additional ADGRB1 (Adhesion G Coupled Receptor B) interactions were recognized, IHA- R132H-Dox+ cells also had these interactions but coverage values was smaller, so they had not shown in **Figure 4.8**. TRIM 28 expression was lower than IHA-R132H-Dox cells as determined in IGV_2_5_0.

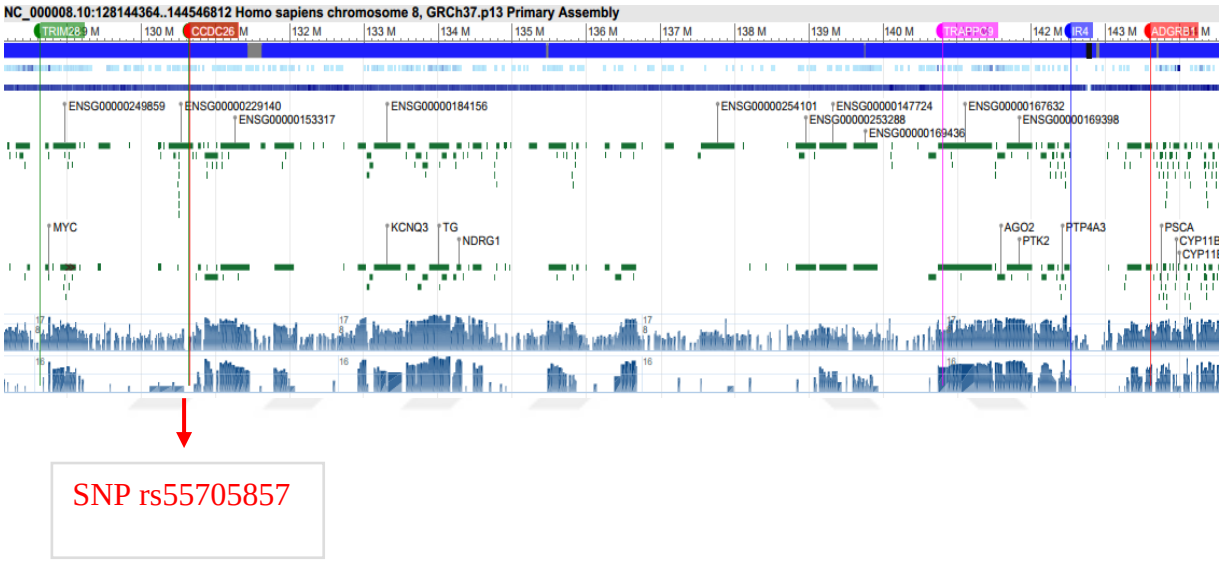

Figure 4.12: (IHA-wt- Dox+) Range is between chr8: 128144365:144546812. Six interacted regions were identified and labeled on image. Two of which were in CCDC26 genomic region, TRIM28 was one of interacted region, one was located in TRAPPC9 (transport protein particle complex 9), there were two additional regions and IR3 was located on 8:142534627-142535775 and last one was in genomic region of ADRGB1 gene. Regions were labeled on NCBI Genome Data Viewer.

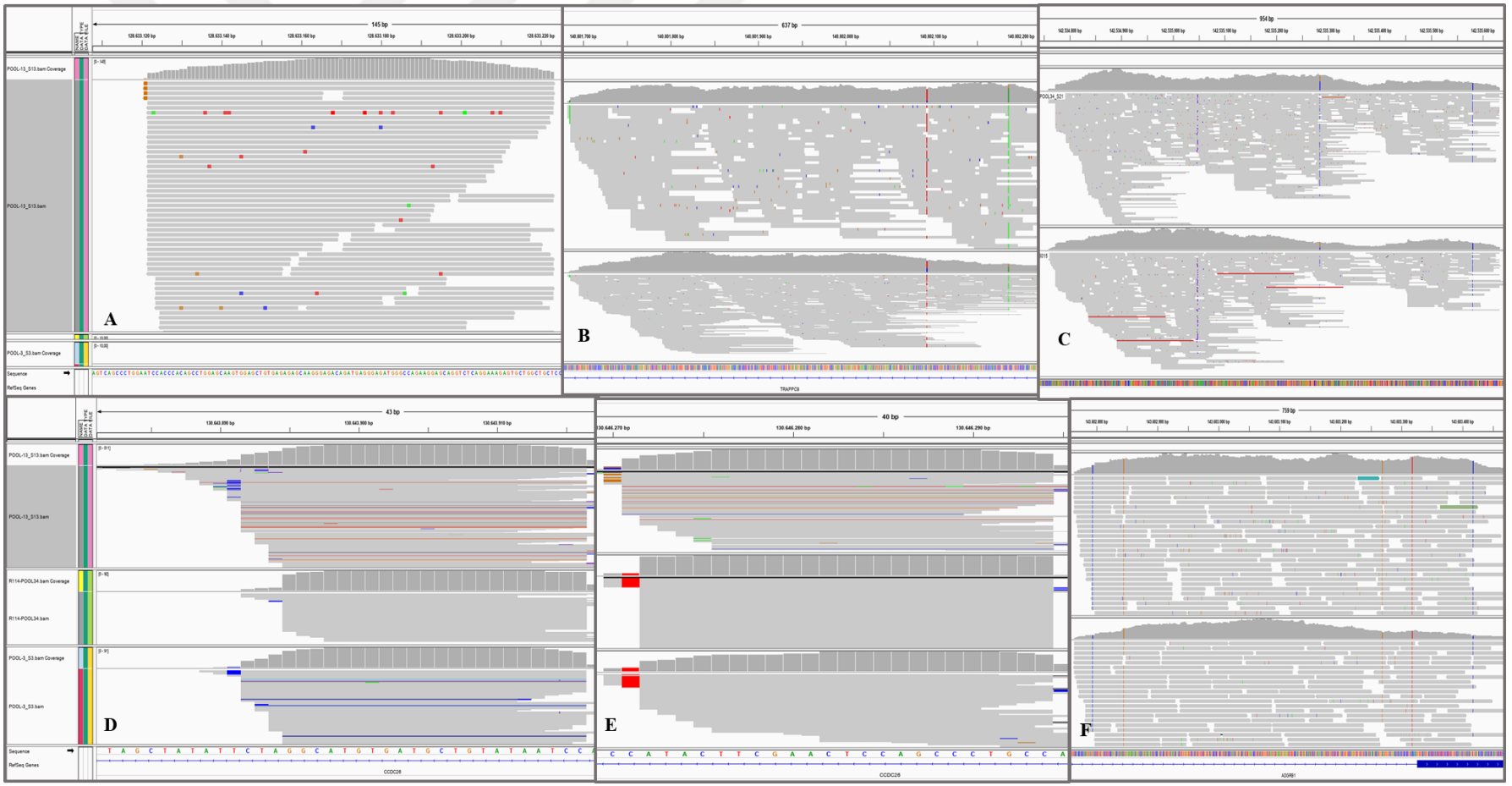

Figure 4.13: IHA-wt-Dox + IGV 2_5_0 interaction images are shown in figure. Interaction of six region, found in IGV, were indicated. A: 128633047-128633307 (TRIM28), B: chr8: 140801585-140802361 (TRAPPC9), C: chr8:142534627-142535777 (IR4), D: chr8:130643881-130643923 (CCDC26), E: chr8: 130646266-130646305 and F: 143602736-143603498 (ADGRBI).

Fifthly, IHA-empty-Dox- cells were analyzed and seven interacted regions were determined. Established regions were marked on NCBI Genome Data Viewer as shown in **Figure 4.14** and IGV2_5_0 views of a couple of interacted regions were indicated in **Figure 4.15.** As differently, two different regions were determined far 12 Mb away risk region, which was near to IR4 found in IHA-wt cells. ADGRB1 (Adhesion G Coupled Receptor B) interactions was recognized again. TRIM 28 expression was almost equal to IHA-wt Dox- cells as determined in IGV_2_5_0. Both Dox- and Dox+ IHA-wt cells were compared for interacted regions in **Figure 4.16.**

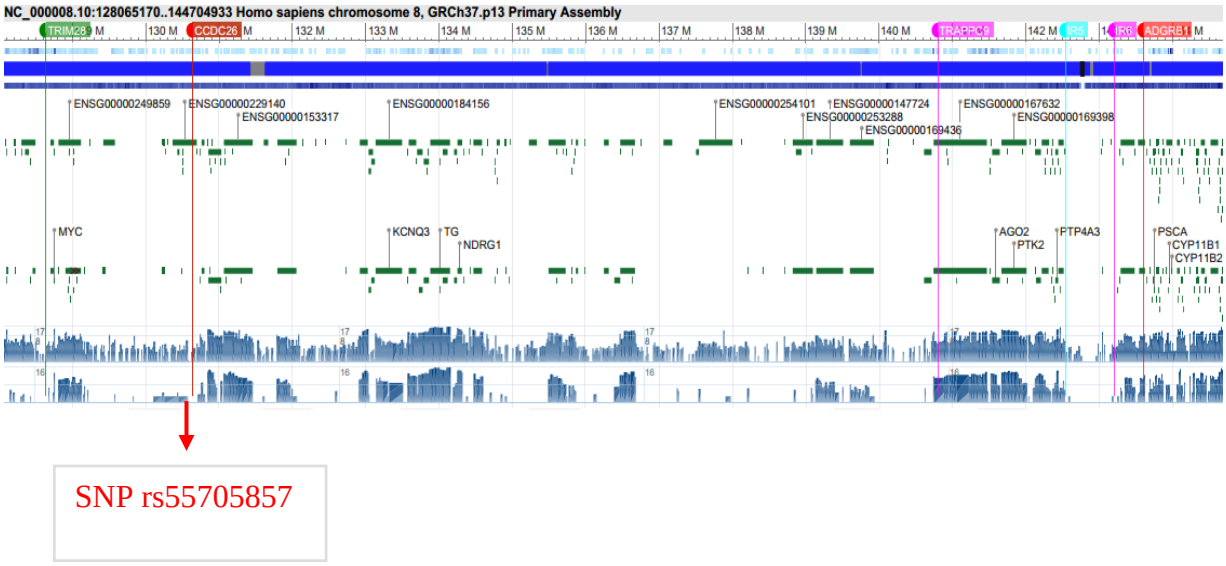

Figure 4.14: Figure indicates IGV_2_5_0 analysis of IHA-empty-Dox- cells. Shown range is between chr8: 128108992:145049899. Seven interacted regions were marked on NCBI Genome Data Viewer. One region was TRIM28 and two of them were in CCDC26. Other was in TRAPPC9 (transport protein particle complex 9), there were two additional interacted regions and IR5 was located on 8:142534727-142536923, IR6 was located at chr8: 143206957-143211349. Last one was in genomic region of ADRGRB1 gene.

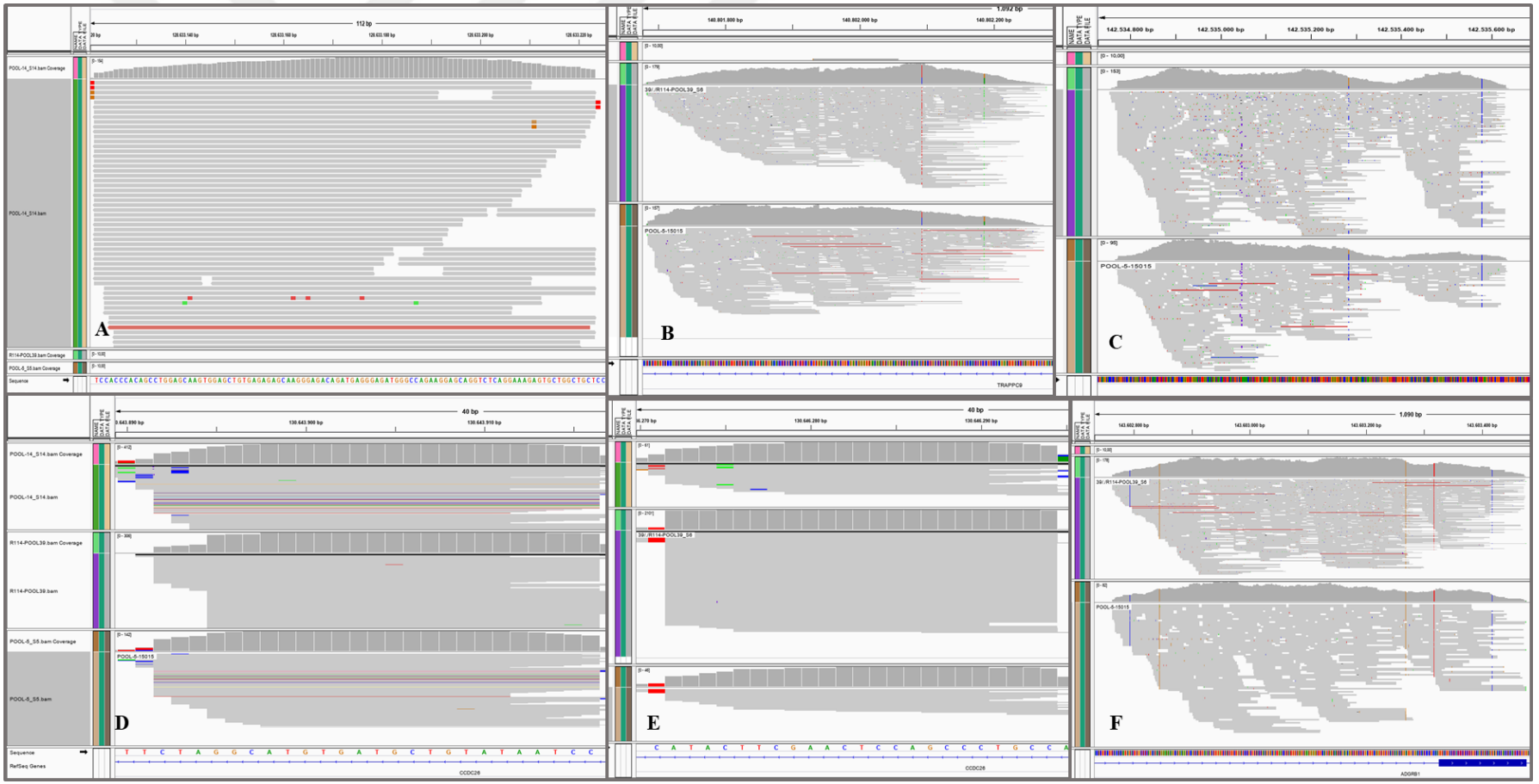

Figure 4.15: IHA-empty-Dox- images of IGV 2_5_0 are shown in figure. Interaction of six region, found in IGV, were indicated. A: 128633047-128633307 (TRIM28), B: chr8: 140801585-140802361 (TRAPPC9), C: chr8:142534727-142536923 (IR5), D: chr8:130643881-130643923 (CCDC26), E: chr8: 130646266-130646305 (CCDC26) and F: 143602736-143603498 (ADGRBI).

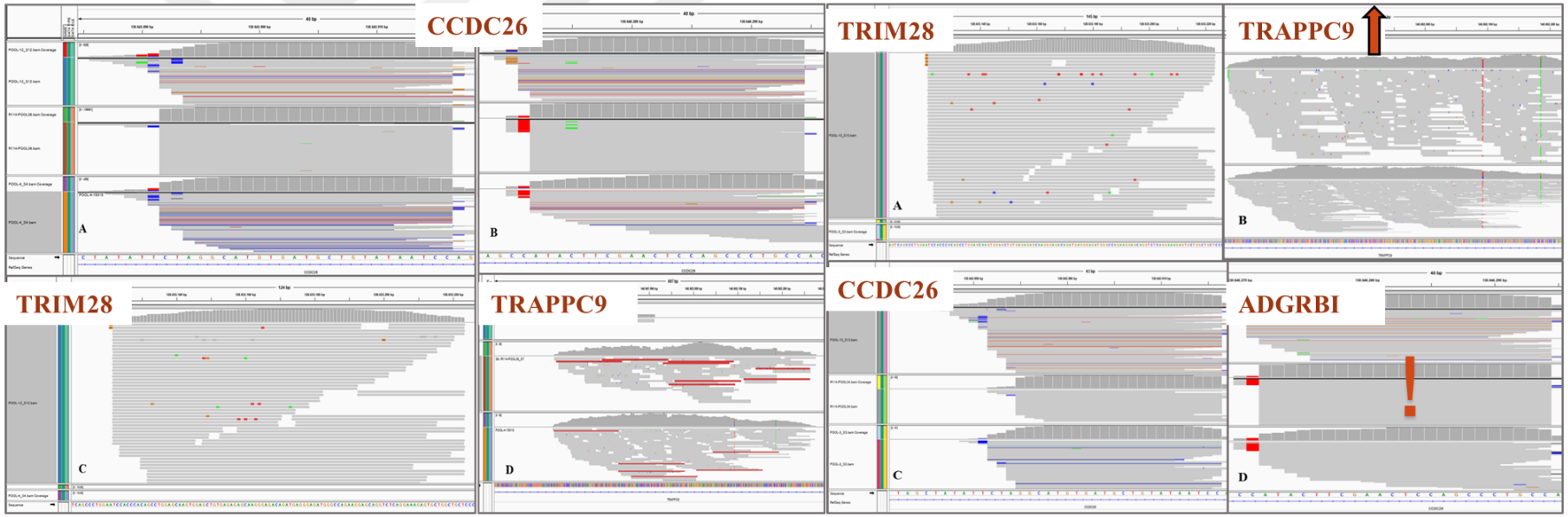

Figure 4.16: Figure shows the some differences and similarities between Dox- and Dox+ IHA-wt cells. Differentially interacted MYC regulator region (TRIM28) was shown again in both Dox- and Dox+ cells. Interactions of TRAPPC9 were shown as increased in Dox+ IHA-wt cells. Differentially ADGRBI expression was observed for Dox+ IHA-wt cells.

Sixthly, analysis of IHA-empty-Dox+ cells were completed. Interacted regions were labeled on NCBI Genome Data Viewer as shown in **Figure 4.17** and IGV2_5_0 views of a interacted regions were shown in **Figure 4.18.** For empty vector included cell lines, there was not significant between dox+ and dox- cells. Therefore, interacted regions were almost the same with IHA-empty-dox – cells. Differences were only related to bam coverage values.

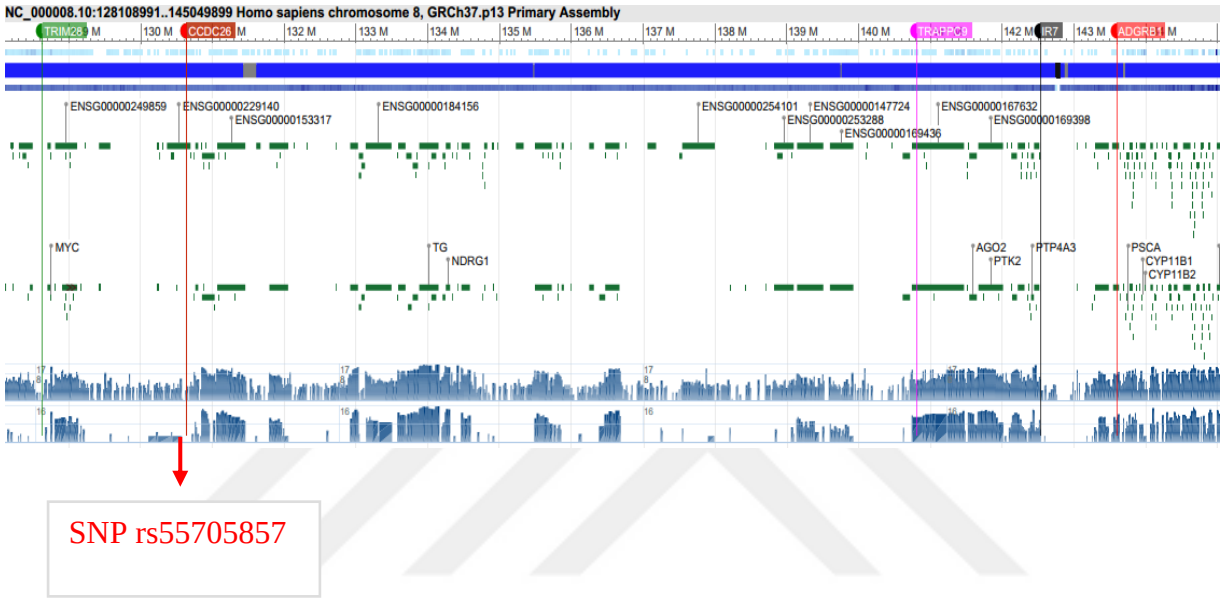

Figure 4.17: Figure demonstrates IGV_2_5_0 analysis of IHA-empty-Dox+ cells. Shown range is between chr8: 128108992:145049899. Six regions were marked on NCBI Genome Data Viewer. One region was TRIM28 and two of them were in CCDC26 as all other. Third was in TRAPPC9 (transport protein particle complex 9), and one additional interacted regions and IR7 was located on 8:142534642-142536837. ADRGRB1 gene was the last one as interacted region in scanned genomic area.

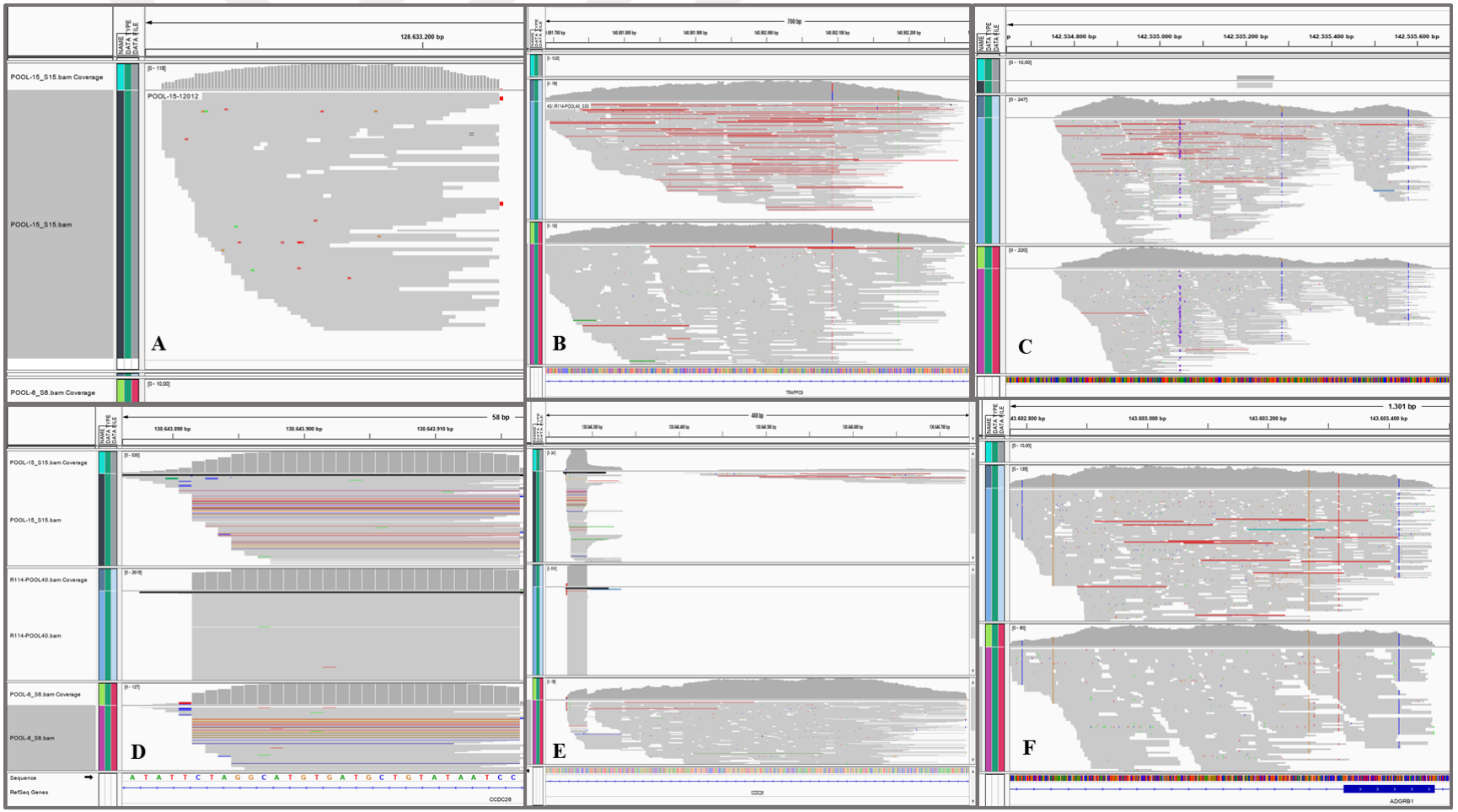

Figure 4.18: IHA-empty-Dox+ images of IGV 2_5_0 are indicated in figure. Interaction of six region, found in IGV, were indicated. A: 128633047-128633307 (TRIM28), B: chr8: 140801585-140802361 (TRAPPC9), C: chr8:142534642-142536837 (IR7), D: chr8:130643881-130643923 (CCDC26), E: chr8: 130646266-130646305 (CCDC26) and F: 143602736-143603498 (ADGRBI).

Lastly, U87 and HEK-293T cells were analyzed. These cell lines were used as kind of control cell lines. As expected, U87 cell line showed too many interactions in genome and HEK-293T cells did not show any interaction except regions where around restriction sites of genomic region where primer sequences aligned. So only some of interactions of U87 cell line was shown in **Figure 4.19.** To understand details of interactions and to compare with kind of non-brain cells, some images of same genomic region of HEK-293T and U87 cell lines were shown in **Figure 4.20 and Figure 4.21** obtained by IGV_2_5_0.

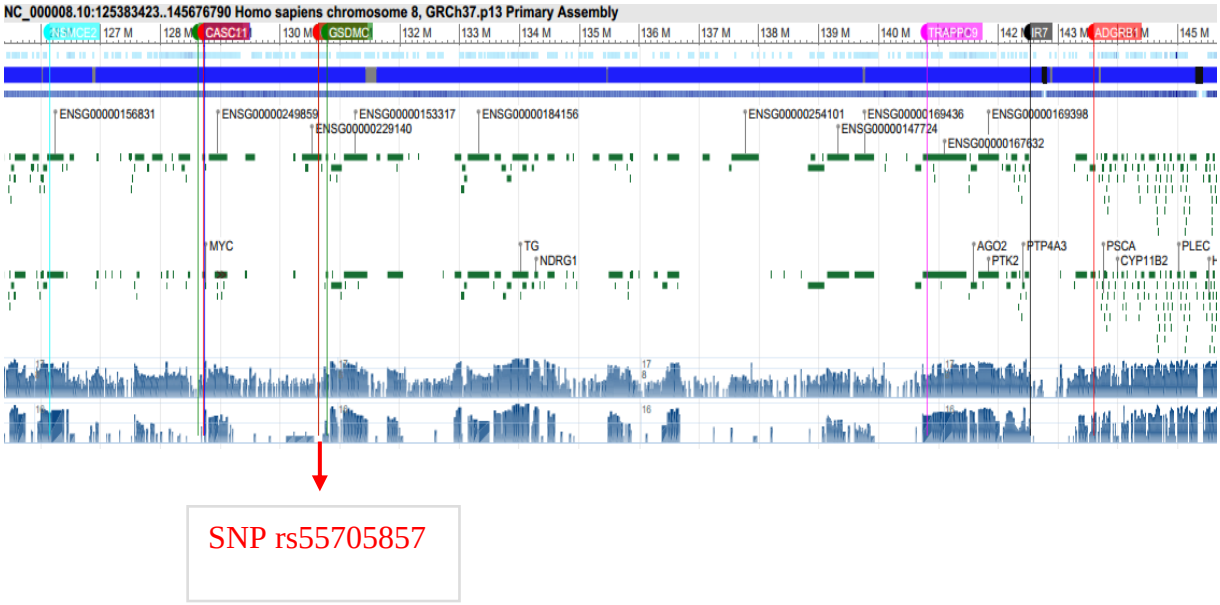

Figure 4.19: Figure shows the couple of example of interacted regions of U87 cell line. Range of analyzed area was between on chromosome 8 from 125383424 to 145676790. Shown regions are that NSMCE2, CASC21, CASC11, CCDC26, GSDMC, TRAPPC9 and ADGRB1 and there were additional interacted regions (mostly in noncoding region) had not been shown.

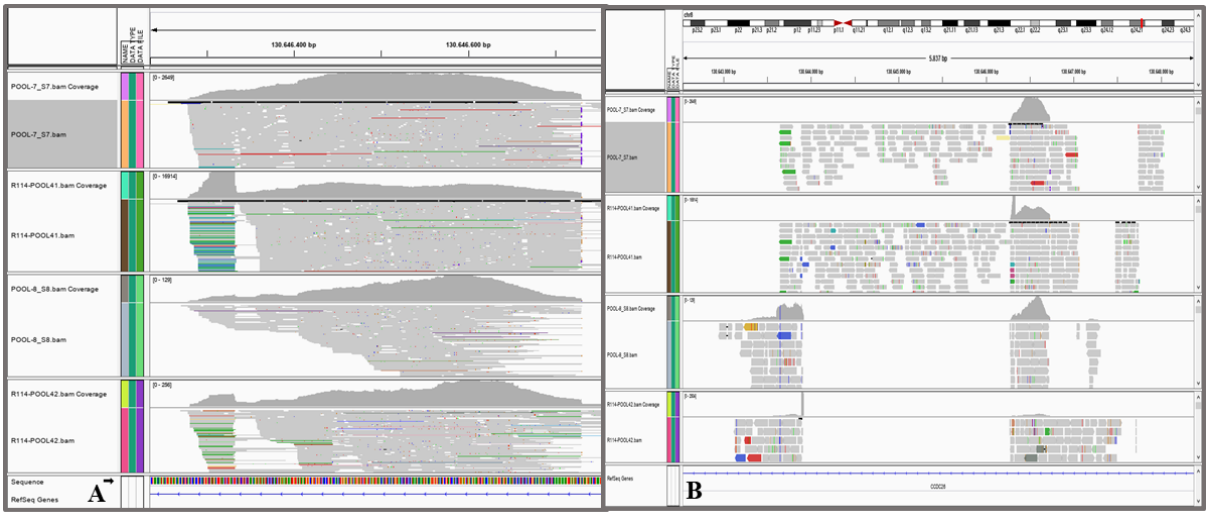

Figure 4.20: Figure shows common interaction regions of U87 and HEK 293-T cell lines by using IGV_2_5_0. Figure A shows the interactions near the risk site in CCDC26. This location was identic for all other cell types that we used. Figure B shows the different interactions where in CCDC26 region. Upper two line indicates the interactions of two replicates of U87 cell line and the lower two lines indicates the two replicates of HEK-293T cell line.

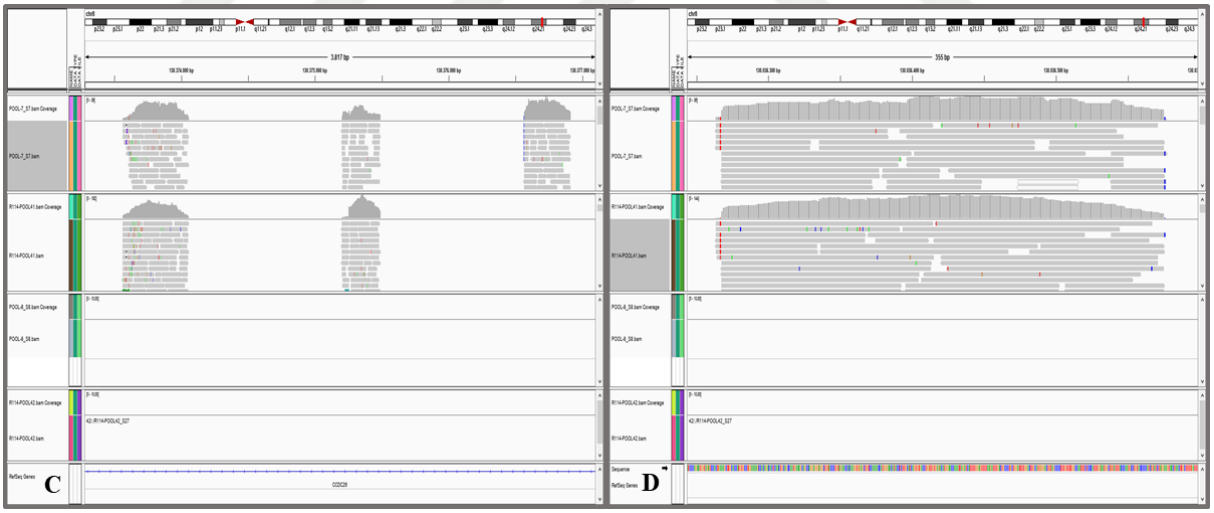

Figure 4.21: Figure indicates the two examples of differences of interacted region between glial cells (U87) and non-glial cells (HEK-293T). Shown both regions are located at 8q24.21 region. When upper two lines show the interactions of U87 cell line, the following two lines indicate that HEK-293T cell do not interact in the same region.

4.5 Selection of Transfected of IPSCs Colonies and Genotyping Results

After puromycin selection of transfected IPSCs, a few colonies could be observed as shown in **Figure 4.20.**

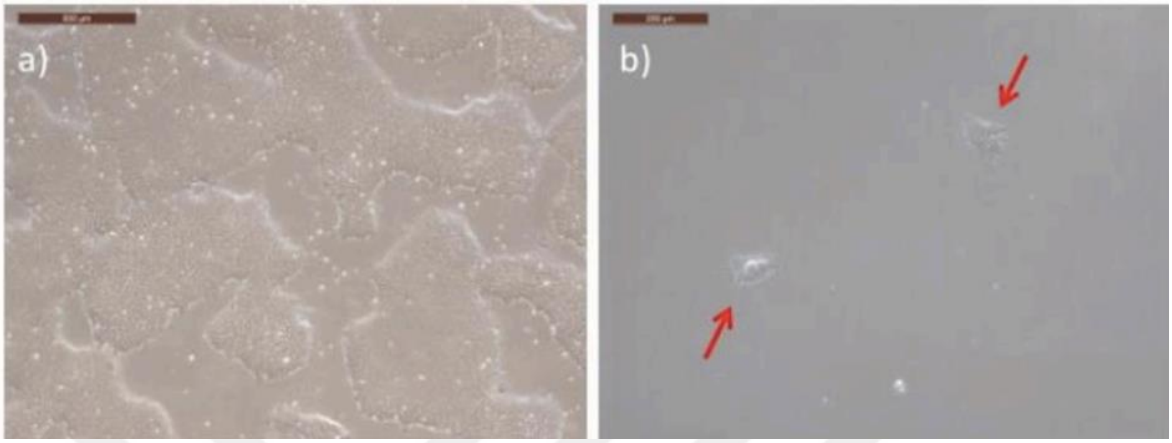

Figure 4.22: Puromycin selection of transfected IPSCs colonies. a) In 48 hours, transfected IPSC colonies were cultured to allow transient expression of puromycin resistance. 0.1 ug/ml puromycin was then applied for an additional 48 hours. b) Only a few colonies were observed after the selection of puromycin.

After selection, IPSCs colonies were isolated and these colonies were genotyped to indicate homozygous point mutation insertion at SNP rs55705857. A homozygous clone was obtained by sequencing as shown in **Figure 4.21.**

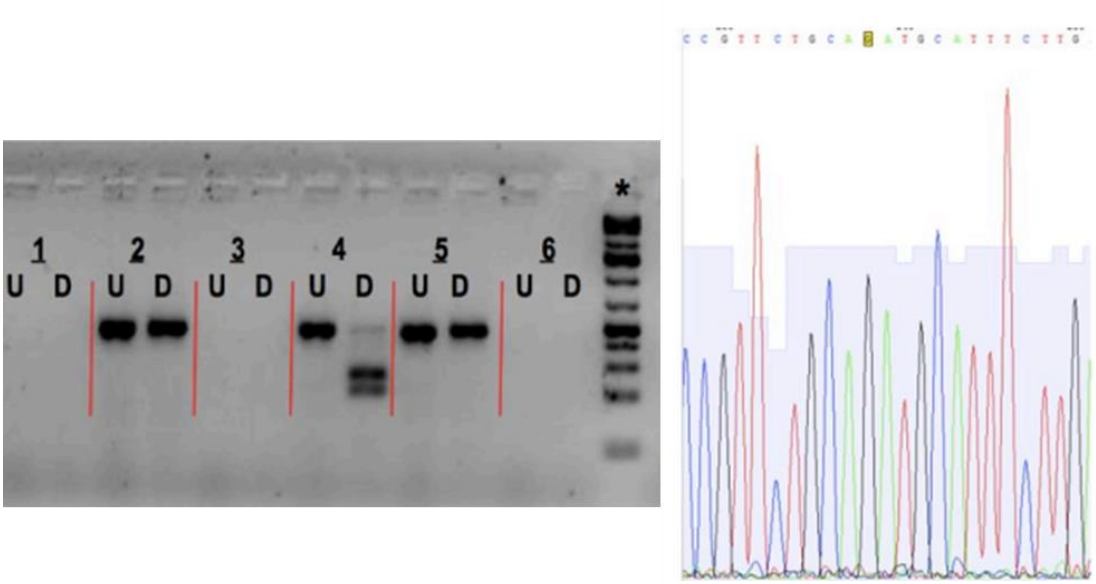

Figure 4.23: Genotyping of rs55705857-GG IPSC clone. Gel image shows the Clone 4 have homozygous G allele and sequence result support agarose gel view.

4.6 Comparison of MYC expression of IPSC-AA and IPSC-GG Cells

When attempting to determine the acting mechanism of rs55705857, MYC was the one of the most possible indirectly interacting region. Thus, CRIPSR/Cas9 edited IPSCs were analyzed using qPCR to indicate MYC expression differences while risk allele exist in the genome. In addition, when these cells were compared, MYC expression was almost 70 times more than as shown in **Figure 4.22.**

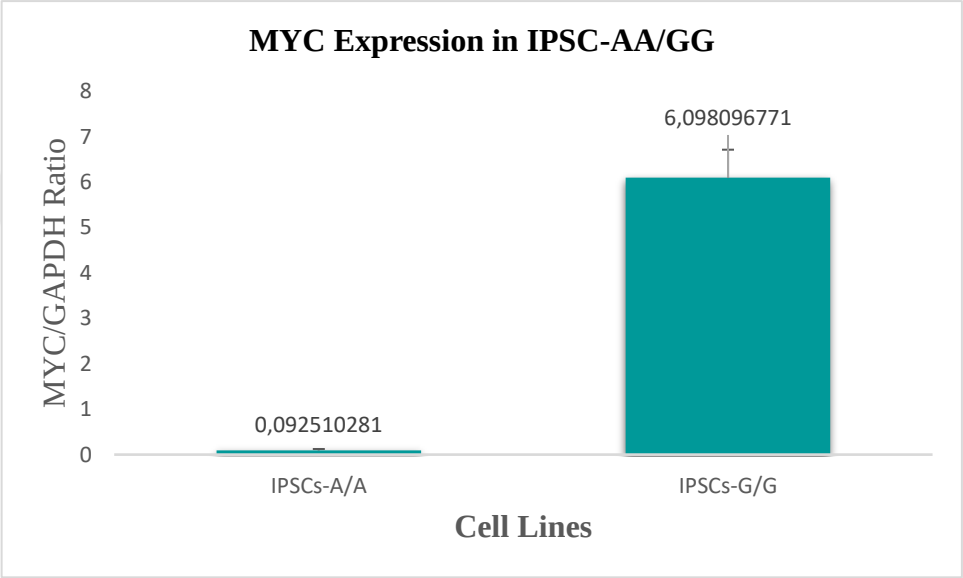

Figure 4.24: Figure indicates the comparison of MYC expression level in IPSC-AA/GG cells. MYC expression in IPSC-GG cells was nearly 70 times more than IPSC-AA cells.

4.7 IDH-R132H Induced Transcriptome Changes in IHA Cells

To understand effects of IDH-R132H mutation, RNA-Seq analysis of astrocyte transcriptomes was performed with 2-HG treated IHA-R132H cells and un-treated IHA-R132H cells as control. Control cells provided to inhibit leaky effects of IDH expression. According to results 446 genes showed changes more than 2 times when $p < 0,05$. The first 60 genes showing the most significant change were shown in the **Table 4.1**.

Table 4.1: Table shows the changes in 2-HG dependent gene expressions of IHA cells.

Gene name	Gene ID	fc	pval
LAP3	150189	53,26123632	6,1983E-05
GPR108	98490	5,227485855	0,000129156
GOT2	76302	61,97293388	0,000146939
KIAA1731	35690	2,194799991	0,000202771
PLK1S1	126010	6,162773861	0,0002197
CALR	100280	584,5152767	0,000529763
NFYC	5007	9,836738478	0,000564988
CTNNB1	138852	4,669814494	0,00062893
ZNF638	114344	7,417601008	0,000789345
ARHGEF40	54511	2,885171912	0,0008372
FBXO3	29059	4,398493934	0,00093578
BABAM1	101250	7,588073562	0,000992461
TAB1	135121	3,793656734	0,000992493
NADSYN1	33954	3,585271842	0,001088916
SEC31A	152735	29,28895456	0,001143202
MYL6	44665	52,47541381	0,00114638
ZNF510	197285	4,451734214	0,001204527
UBL5	99169	145,6781191	0,001206378
C1orf109	4605	4,348389734	0,001263087
BLM	68695	4,803497948	0,001272667
TTPAL	127639	11,69664657	0,001293927
LRRC57	63720	2,304613045	0,001552872
TIPIN	65936	9,234885866	0,00159818
RPS16	104432	16,94006444	0,00160671
ADAL	63835	3,284814452	0,001692306
PRRC2A	168726	4,770232252	0,001805967
DHX57	112479	3,550102212	0,001980015
NLN	159367	6,297041467	0,001988192
MRPL27	88230	33,25422827	0,002069363
RBM42	103318	31,87384351	0,002078874
UBAP1	194792	5,643493007	0,002293911
CWC22	120355	12,81821157	0,002304885
C11orf1	36571	5,709192859	0,002327029
NPIPA7	72439	4,955135096	0,002353596
ROMO1	126992	4,844474116	0,002440544
STRIP1	9337	2,718190191	0,002631141
CCT3	12702	118,8227029	0,002638929
COPS2	64475	2,88694819	0,002697914
CARM1	99575	18,47295487	0,002753675
USP1	7028	32,83157102	0,002816057
CRYL1	50931	6,870905608	0,002962089
ARAP1	34259	2,572833054	0,002995022
ARHGAP12	20308	3,98972646	0,003184172
ASCC2	133686	4,932535766	0,003261901
EIF3K	104161	3,164468436	0,003445189
ZNF227	105691	5,123259356	0,003446282
MEF2D	12772	6,742916188	0,003578036
POFUT2	131447	12,3008742	0,003618181
VAMP7	225975	17,22433545	0,003707692
SH3PXD2B	165243	4,7170632	0,003911682
COPE	101773	2,930029089	0,004044012
HMGA1	169653	2,618120734	0,004141891
STK19P	169107	2,996578588	0,004295618
DNM2	99546	2,895231387	0,004305744
EPG5	95003	3,435571953	0,004414727
ATP5I	148850	19,38391535	0,004518054
OSGEPL1	120671	4,503249929	0,004541286
ARHGAP21	19933	5,454257349	0,004606321
BTF3L4	6366	16,62047839	0,00461357

After that, Enrichr, a web-based bioinformatics tool, was used to understand which processes, pathways and molecule types were enriched in these genes. Enrichr function analyzed the protein-protein interactions of transcription factors controlling these genes, and list of the most significant transcription factors were listed in **Table 4.2** and shown in **Figure 4.23.**

Table 4.2: Table indicates the Enrichr results of PPI enrichment of transcription factors.

Term	Overlap	P-value	Adjusted P-va	Old P-value	Old Adjusted Z-score		Combined Score
MYC	**24/957**	**8,7736E-06**	**0,0010275**	**0,00513036**	**0,3809331**	**-1,8490876**	21,53033581
ATF2	11/237	1,352E-05	0,0010275	0,00081215	0,12344613	-1,7978435	20,15627531
SMARCC2	6/114	0,00067417	0,03415811	0,00751842	0,3809331	-1,7158823	12,52941287
SMARCA4	8/219	0,00101375	0,03852249	0,01630373	0,55024478	-1,7988738	12,40161466
TP53	14/628	0,0021761	0,06615349	0,0754904	0,60077088	-1,7940742	10,99807004
ESR1	17/871	0,0030502	0,07095395	0,13339538	0,60077088	-1,7141234	9,929142611
POU5F1	9/338	0,00433118	0,08229244	0,06188306	0,60077088	-1,6471365	8,963577178
SPI1	4/66	0,00326762	0,07095395	0,01810016	0,55024478	-1,4108951	8,075532351
HDAC2	9/387	0,01013825	0,12049409	0,1166497	0,60077088	-1,6754168	7,692575391
AR	7/271	0,01327508	0,13452083	0,10601967	0,60077088	-1,5331011	6,625858163
FOS	6/199	0,01064395	0,12049409	0,07526566	0,60077088	-1,4567481	6,61766285
MEF2C	3/50	0,01109814	0,12049409	0,04067847	0,60077088	-1,0716072	4,823280377
RAD21	6/237	0,02315755	0,18526044	0,1383354	0,60077088	-1,2585655	4,739045431
SMAD2	8/384	0,02682087	0,19413328	0,20405971	0,66813535	-1,3076249	4,731738609
SMARCC1	4/114	0,02152753	0,18178801	0,09060813	0,60077088	-1,2203863	4,684358531

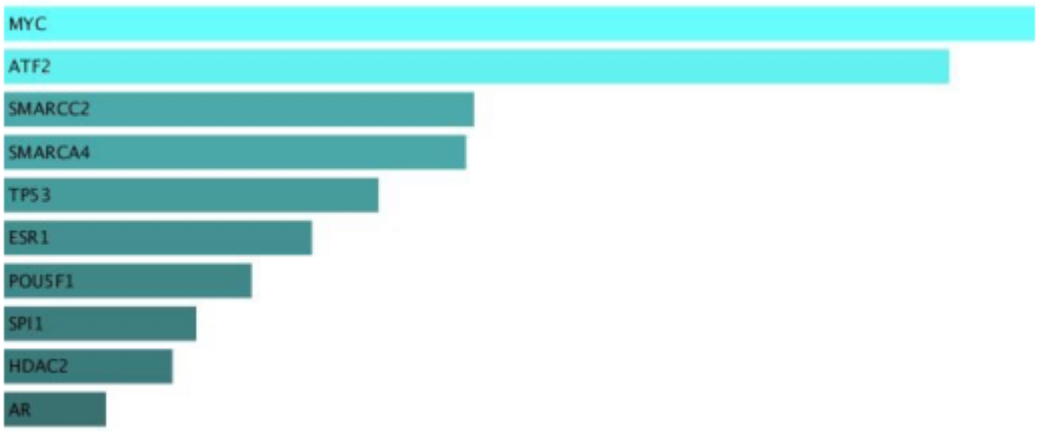

Figure 4.25: Graphical presentation of Enrichr results of PPI enrichment of transcription factors.

When we look at other results of enrichment analysis, TRIM28 was found as the most significant TF as shown in **Figure 4.24.**

Figure 4.26: Figure shows in the Enrichr analysis, the results of the TF-LOF function indicated TRIM 28.

4.8 Genome Edited IPSCs Differentiation for Future Experiments

For future experiments, IPSCs-AA/GG cells were tried to differentiated to ONPC cell lines to analyze effects of rs55705857 by 4C-Seq .First of all, IPSCs-AA/GG cells were cultured on MEF-coated plates to prepare differentiation protocol as shown in **Figure 4.25**.

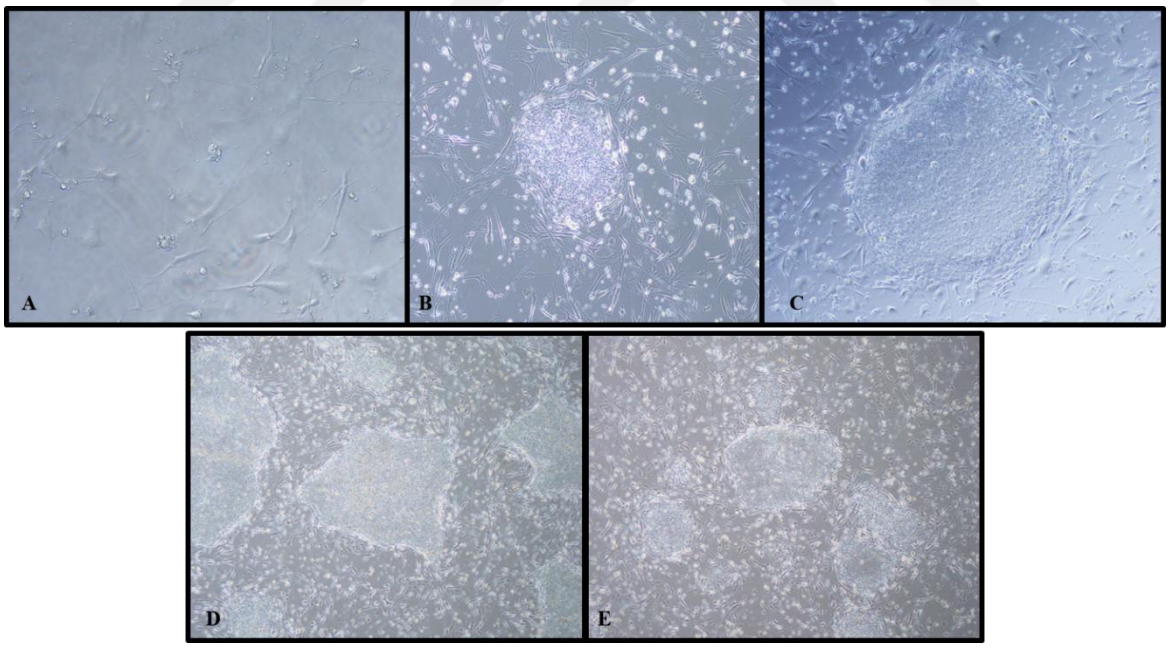

Figure 4.27: Figure shows the cultured IPSCs. A) MEF cells on 0.1% gelatin coated plate. B) IPSC-GG on MEF-coated plate C) IPSCs-AA on MEF-coated plate. Then, cells were proliferated on MEF-coated plates and cultured until colonies were seen by naked eye as shown D) IPSCs-AA and E) IPSCs-GG

Then, cells were passaged to matrigel coated plates and MEF-conditioned media was used until confluency reach to 100% as shown in **Figure 4.26.**

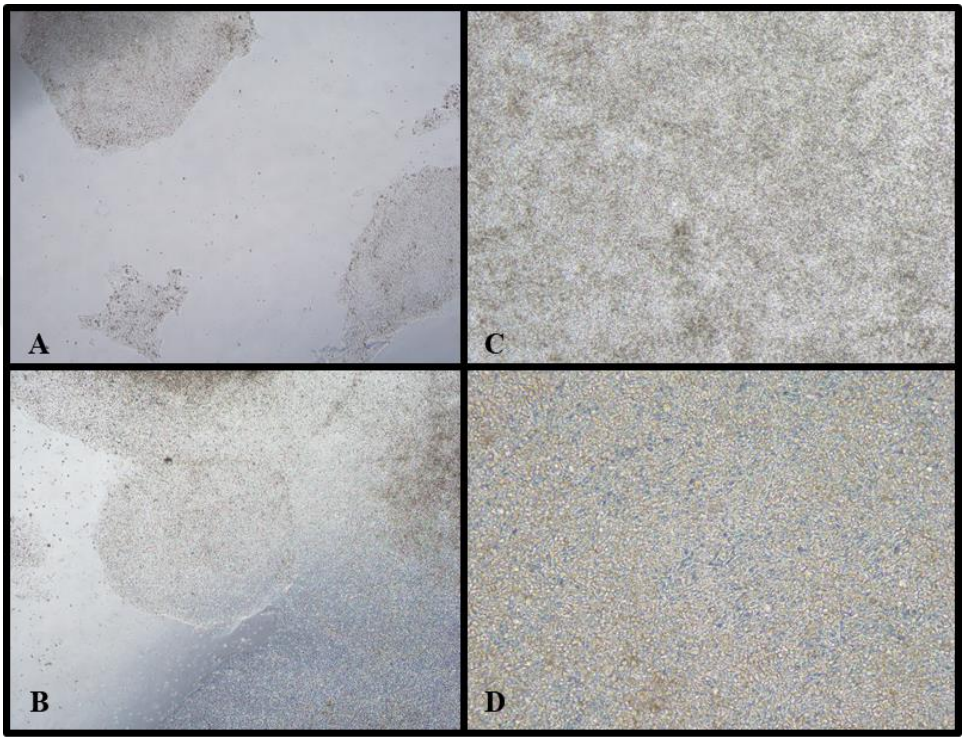

Figure 4.28: Figure shows the IPSCs on matrigel. A and C)IPSCs-AA and B and D shows the IPSCs-GG.

After cells reached to 100 % confluency, neural induction has started and cells has cultured for 8-12 days. During this process, their morphology has started to change as shown in **Figure 4.27.**

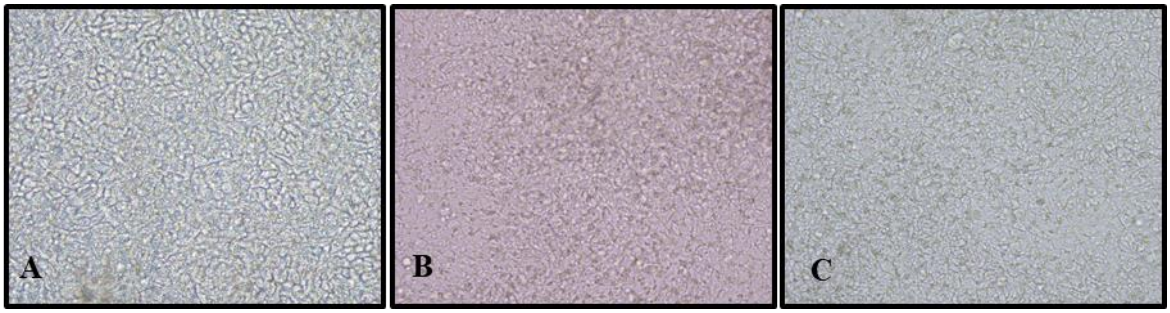

Figure 4.29: Figure shows neural induction process of cells. A) IPSCs-AA, day1, 40X B) IPSCs-AA, day5, 40X, C) IPSCs-AA, day10,40X.

Then cells were passaged to laminin coated plated for proliferation. They has started to grown as colonies as shown in **Figure 4.28.**

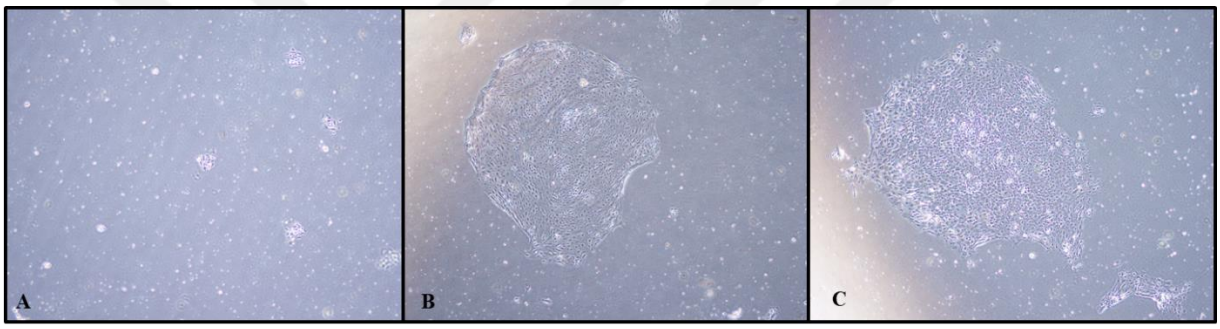

We have reached until proliferation step of differentiation protocol until now.

5 DISCUSSION

IDH1 and IDH2 mutations are the most important mutations for the earliest gliomagenesis steps, in fact they are known as ‘driver mutations’. One of the strongest evidence to support IDH mutations are the earliest mutations seen in the primary tumors, which tend to develop secondary GBMs. IDH mutations are the only mutations that preserved in recurrent brain tumors (Parsons et al., 2008). With the advent of these knowledge, 2016 WHO Classification for brain tumors has upgraded according to the IDH mutation status. IDH mutations are strongly associated with initiation, progression and malignancy of brain tumors (Reifenberger et al., 2016).

2-HG is known oncometabolite of IDH mutations that cause to alterations in DNA and histone methylations by inhibition of demethylases (Yan et al., 2009). While gene expression and cell differentiation change, epigenome and transcriptome of cells are reshaped due to changes in the methylation level in the cell (Yokomori, Pile, Brait, Mellor, & Raineri, 2018). However, the number of studies in which these changes are associated with genetic susceptibility is not sufficient, so, our knowledge of the glioma susceptibility mechanisms is limited.

Completed GWAS studies have shown that the 8q24.21 region is the most effective risk locus for glioma susceptibility. In this region, the most strongly associated SNP is defined as rs55705857 (Jenkins et al., 2012). Although many glioma risk regions have been identified to date, their molecular mechanism has still not been fully elucidated (Kinnersley et al., 2018). Until this project, it has not been clear how SNP rs55705857 provides a genetic predisposition to glioma formation. Because this SNP rs55705857 localizes in the gene desert area long-intergenic intronic region.

It is thought that the known mutations associated with gliomas and the risk regions found in GWAS studies may result in secondary and tertiary mutations on the genome, as well as alterations in chromosome conformation. Therefore, in this study, we tried to show the action mechanism of rs55705857-G risk allele and the effect of IDH-R132H mutation.

For the beginning, in the presence and absence of IDH1-R132H mutation, interactions in and around 8q24.21 were investigated by 4C-Seq method and 2-HG effects on IHA-R132H cells were characterized by RNA-Seq. Because three-dimensional organization of chromatins and long-range interactions are important to understand mechanism of specific regions. By the help of this method, not only indicate known biologic process, but also shows the novel biologic phenomenon to understand genomic organization (Grob & Cavalli, 2018).

As a result of our 4C-Seq data, a large portion of the readings, as expected, are located at both ends of the approximately 2000 base pairs region of CCDC26 containing the rs55705857 locus, between the used restriction enzymes as shown in Figure 4.6 A,B; Figure 4.8 B,C; Figure 4.10 A, B; Figure 4.12 D, E; Figure 4.14 D, E and Figure 4.18 A. On the other hand, the interaction on the genome with five noncoding regions (labeled as IR1, IR2, IR3, IR4 and IR5) and four different encoded regions were found that have not been established in databases .Interaction regions was different between cell types and repeats. This has been shown, as

previously mentioned in the literature that the 3D organization of the genome may vary depending on the experimental conditions and cell types, especially for long-range interactions (Matelot & Noordermeer, 2016). Additionally, chosen restriction enzymes and PCR conditions may affect interaction results of three dimensional structure of chromosome (Z. Zhao et al., 2006).

One of the interaction regions was an interesting finding. This region is approximately 2.1 Mb away from the risk locus. The area is located at the chr8: 128633170 (hg19), as shown in figure A for all astrocyte cell lines. Interaction was strongly observed for all three astrocyte cell lines, both in the presence and absence of doxycycline. What is even more interesting is that this region is being mapped in the USCS Genome Browser to be a regulatory region that controls the MYC gene and also mediated as binding target of a well known receptor transcription factor as TRIM28/KAP1. In addition, MYC was found the most significant transcription factor in the results of the PPI enrichment analysis as shown in Table 4.2 suggest that the mechanism of action of SNP rs55705859 controls MYC expression through this remote interaction.

When we look at the other two interactions that are common in astrocytes, TRAPPC9 and KCNK9 genes were observed. TRAPPC9 encodes a protein to take role in NF-kappa-B signaling and mutations in this gene take role in brain malformation and intellectual disability (Marangi et al., 2013). KCNK9 has function as a pH- dependent potassium channel. Overexpression of this gene was associated with the number of human carcinoma that was related to some growth factors and HIF1A in tumor cells (Mu et al., 2003). 4C-Seq results have demonstrated increase in interactions of SNP rs55705857 in Dox + IHA cells. It has already known that, 2-HG is related to HIF1A expression in gliomas indirect way. So, maybe increased amount of 2-HG in Dox positive cells may cause to interaction of these genes. However, in literature there has not been established relations between these genes and gliomas. So, these genes can be analyzed by other chromosome conformation capture techniques to verify results.

Lastly, found interacting region was ADGRB1 gene refers to brain specific angiogenesis inhibitor. It is clear that, angiogenesis is essential for growth of solid tumors. ADGRB1, also known as BA1 gene, include “functional p53 binding site” where intronic region. wt-p53 induces expression of BA1 gene (Mori et al., 2002). When we look at coverage values of interactions, it can be indicated that, interaction between SNP rs55705857 and BA1 gene was

lower in IHA-R132H dox+ cell. The reason may be that the expression of this gene is changing in the presence of 2-HG and changing interactions can also trigger glioma development and malignancy, as it affects the suppressor task of the gene. However, as mentioned before there are too many parameters to prepare 4C library and fixation time and concentrations, chosen enzymes, experiment conditions and so on can cause differences in many sequencing of same samples. Because each step has the trick, and library preparation is long process. So, to be ensure that every step is performed correctly and each step should be checked to continue. It was advantage to use IHA cells, because they have heterozygous risk allele of rs55705857, this helped to see more of the expected regions. While, all analysis were performed HEK-293T cell line was used to understand background interactions of genome and U87 cell line was used to understand differences between GBMs and astrocytomas.

For continuous part, qPCR analysis of IPS cells, we have created with CRISPR/Cas9 genome regulation and only change in rs55705857 locus, were completed. qPCR results in almost 70 fold increased MYC expression in the risk allele including IPSC-GG cell line. This result strongly supports the hypothesis that the rs55705857 allele in the risk locus has a functional role.

After obtaining information on the possible effects of the IDH1-R132H mutation in astrocytes and possible action mechanism of SNP rs55705857 risk allele, we would like to see the effect of the SNP rs55705857 risk allele from stem cell to neural progenitor cells. Therefore, differentiation protocol of IPSCs to ONPC was tried to perform by using genome edited IPSCs-AA/GG cell lines. However, we had some problems in this differentiation process and could not complete this process, and we will try again this protocol and after differentiation these cell lines could be used for future studies because we have already shown that presence of SNP rs55705857 risk allele cause to 70 times more expression of MYC.

6 CONCLUSIONS AND FUTURE PERSPECTIVES

Overall, for the first time in this study, we have shown that the rs55705857 risk allele interacts with a distal regulatory region that controls MYC expression in astrocytes, which are considered to be among the possible origin cells of the gliomas. In addition, the identification of genes and regions where interaction is possible leads to future studies. .For the future studies, determined regions can be analyzed in detail by using differentiated IPSCs-AA/GG cell lines and different methods can be tried on the same cell lines to make sure the regions found. At the end, disease modeling of gliomas could be formed by using IPSCs cell line. The novel interactions found will provide new treatment methods and new possibilities for patient-specific treatments.

7 REFERENCES

Cohen, A. L., Holmen, S. L., & Colman, H. (2013). IDH1 and IDH2 mutations in gliomas. *Current Neurology and Neuroscience Reports*, *13*(5), 1–7. https://doi.org/10.1007/s11910-013-0345-4

Dang, L., White, D. W., Gross, S., Bennett, B. D., Bittinger, M. A., Driggers, E. M., … Su, M. (2009). Cancer-associated IDH1 mutations produce 2-hydroxyglutarate. *Nature*, *462*(7274), 739. https://doi.org/10.1038/nature08617

Dekker, J. (2006). The three "C" s of chromosome conformation capture: Controls, controls, controls. *Nature Methods*, *3*(1), 17–21. https://doi.org/10.1038/nmeth823

Dekker, J., Rippe, K., Dekker, M., & Kleckner, N. (2002a). Capturing Chromosome Conformation. *Science*, *295*(5558), 1306–1311. https://doi.org/10.1126/SCIENCE.1067799

Dekker, J., Rippe, K., Dekker, M., & Kleckner, N. (2002b). Capturing Chromosome Conformation. *Science*, *295*(5558), 1306–1311. https://doi.org/10.1126/SCIENCE.1067799

Enciso-Mora, V., Hosking, F. J., Kinnersley, B., Wang, Y., Shete, S., Zelenika, D., … Houlston, R. S. (2013). Deciphering the 8q24.21 association for glioma. *Human Molecular Genetics*, *22*(11), 2293–2302. https://doi.org/10.1093/hmg/ddt063

Gavrilov, A., Eivazova, E., Pirozhkova, I., Lipinski, M., Razin, S., & Vassetzky, Y. (2009). Chromosome Conformation Capture (from 3C to 5C) and Its ChIP-Based Modification. *Springer*, *567*, 171–188. https://doi.org/10.1007/978-1-60327-414-2

González-Castro, T. B., Juárez-Rojop, I. E., López-Narváez, M. L., Tovilla-Zárate, C. A., Genis-Mendoza, A. D., Pérez-Hernández, N., … Rodríguez-Pérez, J. M. (2019). Genetic Polymorphisms of CCDC26 rs891835, rs6470745, and rs55705857 in Glioma Risk: A Systematic Review and Meta-analysis. *Biochemical Genetics*, (0123456789). https://doi.org/10.1007/s10528-019-09911-7

Grandy, R., Tomaz, R. A., & Vallier, L. (2019). Modeling Disease with Human Inducible Pluripotent Stem Cells. *Annu. Rev. Pathol. Mech. Dis. 2019*, *14*, 449–468.

https://doi.org/10.1146/annurev-pathol-020117

Grob, S., & Cavalli, G. (2018). Technical Review: A Hitchhiker's Guide to Chromosome Conformation Capture, *1675*. https://doi.org/10.1007/978-1-4939-7318-7

Hockemeyer, D., & Jaenisch, R. (2016). Induced pluripotent stem cells meet genome editing. *Cell Stem Cell*. https://doi.org/10.1016/j.stem.2016.04.013

Ichimura, K. (2012). Molecular pathogenesis of IDH mutations in gliomas. *Brain Tumor Pathology*, *29*(3), 131–139. https://doi.org/10.1007/s10014-012-0090-4

Illumina. (2018). *MiniSeq System Guide (1000000002695)*. Retrieved from www.illumina.com/company/legal.html.

Iorgulescu, J. B., Torre, M., Harary, M., Smith, T. R., Aizer, A. A., Reardon, D. A., … Perry, A. (2019). The Misclassification of Diffuse Gliomas: Rates and Outcomes. *Clinical Cancer Research*. https://doi.org/10.1158/1078-0432.CCR-18-3101

Jenkins, R. B., Xiao, Y., Sicotte, H., Decker, P. A., Kollmeyer, T. M., Hansen, H. M., … Wrensch, M. R. (2012). A low-frequency variant at 8q24.21 is strongly associated with risk of oligodendroglial tumors and astrocytomas with IDH1 or IDH2 mutation. *Nature Genetics*, *44*(10), 1122–1125. https://doi.org/10.1038/ng.2388

Kinnersley, B., Houlston, R. S., & Bondy, M. L. (2018). Genome-Wide Association Studies in Glioma. *Cancer Epidemiol Biomarkers*. https://doi.org/10.1158/1055-9965.EPI-17-1080

Liu, Y., Shete, S., Hosking, F., Robertson, L., Houlston, R., & Bondy, M. (2010). Genetic advances in glioma: susceptibility genes and networks. *Current Opinion in Genetics & Development*, *20*, 239–244. https://doi.org/10.1016/j.gde.2010.02.001

Louis, D. N., Perry, A., Reifenberger, · Guido, Von Deimling, A., Figarella-Branger, D., Webster, ·, … Ellison, W. (2016). The 2016 World Health Organization Classification of Tumors of the Central Nervous System: a summary. *Springer*. https://doi.org/10.1007/s00401-016-1545-1

Lu, C., Ward, P. S., Kapoor, G. S., Rohle, D., Turcan, S., Abdel-Wahab, O., … Thompson, C. B. (2012). IDH mutation impairs histone demethylation and results in a block to cell

differentiation. *Nature*, *483*(7390), 474–478. https://doi.org/10.1038/nature10860

Madala, H. R., Punganuru, S. R., Arutla, V., Misra, S., Thomas, T. J., & Srivenugopal, K. S. (2018). Beyond brooding on oncometabolic havoc in IDH-mutant gliomas and AML: Current and future therapeutic strategies. *Cancers*, *10*(2). https://doi.org/10.3390/cancers10020049

Malta, T. M., de Souza, C. F., Sabedot, T. S., Silva, T. C., Mosella, M. S., Kalkanis, S. N., … Noushmehr, H. (2017). Glioma CpG island methylator phenotype (G-CIMP): biological and clinical implications. *Neuro-Oncology*. https://doi.org/10.1093/neuonc/nox183

Marangi, G., Leuzzi, V., Manti, F., Lattante, S., Orteschi, D., Pecile, V., … Zollino, M. (2013). TRAPPC9-related autosomal recessive intellectual disability: report of a new mutation and clinical phenotype. *European Journal of Human Genetics*, *21*(2), 229–232. https://doi.org/10.1038/ejhg.2012.79

Matelot, M., & Noordermeer, D. (2016). Determination of High-Resolution 3D Chromatin Organization Using Circular Chromosome Conformation Capture (4C-seq). *Springer*, *1480*(14), 2704–2712. https://doi.org/10.1007/978-1-4939-6380-5_20

Melin, B., Barnholtz, S. J., Wrensch, M., Johansen, C., Il'yasova, D., Kinnersley, B., … Bondy, M. (2017). Genome-wide association study of glioma subtypes identifies specific differences in genetic susceptibility to glioblastoma and non-glioblastoma tumor. *Nature Genetics*, 22. https://doi.org/10.1038/ng.3823

Mori, K., Kanemura, Y., Fujikawa, H., Nakano, A., Ikemoto, H., Ozaki, I., … Arita, N. (2002). Brain-specific angiogenesis inhibitor 1 (BAI1) is expressed in human cerebral neuronal cells. *Neuroscience Research*, *43*(1), 69–74. https://doi.org/10.1016/S0168-0102(02)00018-4

Mu, D., Chen, L., Zhang, X., See, L.-H., Koch, C. M., Yen, C., … Powers, S. (2003). Genomic amplification and oncogenic properties of the KCNK9 potassium channel gene. *Cancer Cell*, *3*(3), 297–302. https://doi.org/10.1016/S1535-6108(03)00054-0

Oktay, Y., Ülgen, E., Can, Ö., Akyerli, C. B., Yüksel, Ş., Erdemgil, Y., … Özduman, K. (2016). IDH-mutant glioma specific association of rs55705857 located at 8q24.21 involves MYC deregulation OPEN. *Nature Publishing Group*.

https://doi.org/10.1038/srep27569

Parsons, william D., Jones, S., Zhang, X., Cheng-Ho Lin, J., Leary, R. J., Angenendt, P., … Kinzler, K. W. (2008). An Integrated Genomic Analysis of Human Glioblastoma Multiforme. *Science, 321*(5897), 1807. https://doi.org/10.1126/science.1164382

Rajaraman, P., Melin, B. S., Wang, Z., McKean-Cowdin, R., Michaud, D., Wang, S. S., … Chanock, S. J. (2012). Genome-wide Association Study of Glioma and Meta-Analysis. *Hum Genet, 131*(12), 1877–1888. https://doi.org/10.1007/s00439-012-1212-0

Reifenberger, G., Wirsching, H.-G., Knobbe-Thomsen, C. B., & Weller, M. (2016). Advances in the molecular genetics of gliomas — implications for classification and therapy. *Nature Reviews Clinical Oncology, 14*(7), 434–452. https://doi.org/10.1038/nrclinonc.2016.204

Rohle, D., Popovici-Muller, J., Palaskas, N., Turcan, S., Grommes, C., Campos, C., … Mellinghoff, I. K. (2013). An Inhibitor of Mutant IDH1 Delays Growth and Promotes Differentiation of Glioma Cells. *Science, 340*(6132), 626–630. https://doi.org/10.1126/science.1236062

Sanson, M., Hosking, F. J., Shete, S., Zelenika, D., Dobbins, S. E., Ma, Y., … Simon, M. (2011). Chromosome 7p11.2 (EGFR) variation influences glioma risk. *Human Molecular Genetics, 11*(14), 2897–2904. https://doi.org/10.1093/hmg/ddr192

Sati, S., & Cavalli, G. (2016). Chromosome conformation capture technologies and their impact in understanding genome function. https://doi.org/10.1007/s00412-016-0593-6

Sati, S., & Cavalli, G. (2017). Chromosome conformation capture technologies and their impact in understanding genome function. *Chromosoma, 126*(1), 33–44. https://doi.org/10.1007/s00412-016-0593-6

Schwartzbaum, J. A., Fisher, J. L., Aldape, K. D., & Wrensch, M. (2006). Epidemiology and molecular pathology of glioma. *Nature Clinical Practice Neurology, 2*(9), 494–503. https://doi.org/10.1038/ncpneuro0289

Shete, S., Hosking, F. J., Robertson, L. B., Dobbins, S. E., Sanson, M., Malmer, B., … Houlston, R. S. (2009). Genome-wide association study identifies five susceptibility loci for glioma. *Nature Genetics, 41*(8), 899–904. https://doi.org/10.1038/ng.407

Shi, Y., Kirwan, P., & Livesey, F. J. (2012). Directed differentiation of human pluripotent stem cells to cerebral cortex neurons and neural networks. *Nature Protocols*, *7*(10), 1836–1846. https://doi.org/10.1038/nprot.2012.116

Simon, M., Hosking, F. J., Marie, Y., Gousias, K., Boisselier, B., Carpentier, C., … Sanson, M. (2010). Genetic risk profiles identify different molecular etiologies for glioma. *Clinical Cancer Research*, *16*(21), 5252–5259. https://doi.org/10.1158/1078-0432.CCR-10-1502

Sonoda, Y., Ozawa, T., Hirose, Y., Aldape, K. D., Mcmahon, M., Berger, M. S., & Pieper, R. O. (2001). Formation of Intracranial Tumors by Genetically Modified Human Astrocytes Defines Four Pathways Critical in the Development of Human Anaplastic Astrocytoma. *Cancer Research*, *53*(1005), 4956–4960.

Tateishi, K., & Yamamoto, T. (2019). IDH-Mutant Gliomas. In *Brain and Spinal Tumors - Primary and Secondary [Working Title]*. IntechOpen. https://doi.org/10.5772/intechopen.84543

Turcan, S., Fabius, A. W. M., Borodovsky, A., Pedraza, A., Brennan, C., Huse, J., … Chan, T. A. (2013). *Efficient induction of differentiation and growth inhibition in IDH1 mutant glioma cells by the DNMT Inhibitor Decitabine*. *Oncotarget* (Vol. 4). Retrieved from www.impactjournals.com/oncotarget

Turcan, S., Makarov, V., Taranda, J., Wang, Y., Fabius, A. W. M., Wu, W., … Chan, T. A. (2018). Mutant-IDH1-dependent chromatin state reprogramming, reversibility, and persistence. *Nature Genetics*, *50*(1), 62–72. https://doi.org/10.1038/s41588-017-0001-z

Turcan, S., Rohle, D., Goenka, A., Walsh, L. A., Fang, F., Yilmaz, E., … Performed, L. G. T. M. S. T. (2012). IDH1 mutation is sufficient to establish the glioma hypermethylator phenotype. *Nature*, *483*(7390), 479–483. https://doi.org/10.1038/nature10866

Van De Werken, H. J. G., De Vree, P. J. P., Splinter, E., Holwerda, S. J. B., Klous, P., De Wit, E., & De Laat, W. (2012). 4C technology: Protocols and data analysis. *Methods in Enzymology*, *513*(JANUARY), 89–112. https://doi.org/10.1016/B978-0-12-391938-0.00004-5

Walsh, K. M., Codd, V., Smirnov, I. V, Rice, T., Decker, P. A., Hansen, H. M., … Genet, N.

(2014). Variants near TERT and TERC influencing telomere length are associated with high-grade glioma risk HHS Public Access Author manuscript. *Nat Genet*, *46*(7), 731–735. https://doi.org/10.1038/ng.3004

Ward, P. S., Patel, J., Wise, D. R., Abdel-Wahab, O., Bennett, B. D., Coller, H. A., … Thompson, C. B. (2010). The common feature of leukemia-associated IDH1 and IDH2 mutations is a neomorphic enzymatic activity that converts α-ketoglutarate to 2-hydroxyglutarate. *Cancer Cell*, *17*(3), 225–234. https://doi.org/10.1016/j.ccr.2010.01.020

Yan, H., Williams, D., Jin, G., Mclendon, R., Rasheed, B. A., Yuan, W., … Bigner, D. D. (2009). IDH1 and IDH2 Mutations in Gliomas. https://doi.org/10.1056/NEJMoa0808710

Yen, K. E., Bittinger, M. A., Su, S. M., & Fantin, V. R. (2010). Cancer-associated IDH mutations: biomarker and therapeutic opportunities. *Oncogene*, *29*(49), 6409–6417. https://doi.org/10.1038/onc.2010.444

Yokomori, K., Pile, L. A., Brait, M., Mellor, J., & Raineri, S. (2018). IDH1: Linking Metabolism and Epigenetics. https://doi.org/10.3389/fgene.2018.00493

Zhao, S., Lin, Y., Xu, W., Jiang, W., Zha, Z., Wang, P., … Xiong, Y. (2009). Glioma-Derived Mutations in IDH1 Dominantly Inhibit IDH1 Catalytic Activity and Induce HIF-1α. *Science*, *324*(5924), 261–265. https://doi.org/10.1126/science.1170944

Zhao, Z., Tavoosidana, G., Sjölinder, M., Göndör, A., Mariano, P., Wang, S., … Ohlsson, R. (2006). Circular chromosome conformation capture (4C) uncovers extensive networks of epigenetically regulated intra- and interchromosomal interactions. *Nature Genetics*, *38*(11), 1341–1347. https://doi.org/10.1038/ng1891

ÖZGEÇMİŞ

Adı, Soyadı; Tutku YARAŞ

Doğum Yılı:	1992
Yazışma Adresi:	KılıçReis Mah. 281 Sokak No:18 Daire:5 Üçyol /Konak/İzmir
Telefon:	5543171352
Faks:	
e-posta:	yaras.tutku@gmail.com

EĞİTİM BİLGİLERİ

Ülke	Üniversite	Fakülte/Enstitü	Öğrenim Alanı	Derece	Mezuniyet Yılı
TR	DEU-IBG	Genom Bilimleri ve Moleküler Biyoteknoloji	MBG	3,75	2019
TR	İYTE	MBG	MBG	2,66	2016

AKADEMİK/MESLEKTE DENEYİM

Kurum/Kuruluş	Ülke	Şehir	Bölüm/Birim	Görev Türü	Görev Dönemi
IBG	TR	İzmir	MBG	Yardımcı Araştırmacı	07/2018-Current

UZMANLIK ALANLARI

Uzmanlık Alanları
• Bacteria culturing, • Cell culturing, • DNA extraction from cell • DNA isolation from blood, • RNA isolation from cell/blood, • Fluorescence microscopy • Protein purification, • Spectrophotometry, • PCR, • Electrophoretic techniques (Agarose, SDS-PAGE), • Transformation, transfection • PDMS preparation, • Gene Cloning, • BRET Analysis, • IPS Cell Culture • Chromatin Conformatin Capture Technique (4C), • RT- PCR

YAYINLARI

SCI, SSCI, AHCI indekslerine giren dergilerde yayınlanan makaleler

Diğer dergilerde yayınlanan makaleler

Hakemli konferans/sempozyumların bildiri kitaplarında yer alan yayınlar
